**Reports of the International Ocean-Colour Coordinating Group**

**IOCCG Report Number 1, 1998**

# Minimum Requirements for an Operational, Ocean-Colour Sensor for the Open Ocean

Report of an IOCCG working group held in
Villefranche-sur-Mer, France, October 6-7, 1997.
Chaired by Prof. André Morel.

*Published by the International Ocean-Colour Coordinating Group (IOCCG), an Affiliated Program of the Scientific Committee on Oceanic Research (SCOR).*

ISSN: 1098-6030 ISBN: 978-1-896246-52-9

*The IOCCG is an international group of experts in the field of satellite ocean colour, which acts as a liaison and communication channel between users, managers and agencies in the ocean colour arena.*

*The IOCCG is sponsored by NASA (National Aeronautics and Space Administration), NASDA (National Space Development Agency of Japan), ESA (European Space Agency), CNES (Centre National D'Etudes Spatiales), JRC (Joint Research Centre, EC), CSA (Canadian Space Agency), AMRS (Alliance of Marine Remote Sensing), and SCOR (Scientific Committee on Oceanic Research).*

*IOCCG Project Office: Bedford Institute of Oceanography, P.O. Box 1006, Dartmouth, Nova Scotia, Canada, B2Y 4A2*

*www.ioccg.org*

# Contents

# 1. Introduction

The forerunner of all ocean-colour satellite sensors, the CZCS (1978-1986), has led to a series of increasingly-sophisticated instruments: MOS, OCTS, POLDER, and SeaWiFS launched in 1996-1997, and MODIS, MISR, OCM, GLI, OCI, OSMI, MERIS, and POLDER-2 scheduled to be launched in 1998-2000. The sophistication, and expected improvements, have mainly consisted in better radiometric performances (in terms of dynamical range and signal-to-noise ratio), and in increased number of spectral channels (from 5 for CZCS up to 36 for MODIS and GLI). Many additional channels are actually devoted to terrestrial vegetation and atmospheric features, since these new instruments are designed to fulfill multipurpose missions. Other kinds of sophistication were also introduced to allow multi-angle viewing capability (POLDER, MISR), and, in addition, to determine the state of polarization of the reflected radiation (POLDER 1 and 2). Such increased complexities in the sensor's design were a response to the demands of the scientific community, and were essentially based on new research objectives or exploratory projects. This goal implies the development of new experimental algorithms, and the definition of new products for the user community.

The views presented in this document are deliberately oriented in the opposite direction, as they deal with a question that could be formulated as follows: Is it possible to satisfy the requirements for an operational ocean-colour mission at low cost based on simple sensors? In particular, is there any possibility of providing useful information if the sensor is operated with a reduced number of spectral channels? If such a minimal set of bands could be identified, a corollary would be to recommend it for inclusion in all sensors, regardless of their other capabilities and of the larger number of channels they may possess. A commonality in the spectral acquisition provides important practical, as well as scientific, advantages. Indeed, it would allow:

- easy intercomparison between sensors, and even radiometric intercalibration in well-defined conditions;
- a full compatibility of operational algorithms for atmospheric correction and derivation of end products;
- a meaningful data merging, at the level of geophysical products (pigment index, aerosol optical thickness) or at the level of the initial quantities (*e.g.*, spectral normalized radiances);
- a long-term continuity of ocean-colour observations, based on stable, entirely comparable, parameters; and therefore
- the building up of a coherent data base for biogeochemical studies and related modeling activities, for physical studies and models (heating rate, mixed layer dynamics), and for climatological purposes involving the radiative budget and the effect of aerosol loading.

Several limitations on, and assumptions about, the subject matter were adopted for the present discussion. It has been postulated that an environmental monitoring program based on ocean-colour observation, and in essence, similar to those in operation for meteorology and for some oceanographic variables (sea-level, for instance), is needed, and must cover the entire open ocean and the coastal zones. Such a monitoring of the marine algal biomass distribution, activity, and impact, is a crucial aim of core programs of the IGBP (JGOFS, GLOBEC, LOICZ, and their successors). It could be performed at low cost by using simple, small and inexpensive sensors. Such an operational system is supposed to rely on dedicated sensors for ocean colour, so that there will be no need for compromises with other kinds of missions when designing the instrument. It would require several identical instruments operating simultaneously in orbit. The deployment of such simple sensors is in no way contradictory to the conception, development and use of more sophisticated instruments, designed for advanced research purposes. Indeed, several sensors will be in simultaneous operation in the near future, with differing capabilities, some complementarity, and a partial planned redundancy. Finally, the issue of algorithms, beyond the scope of the present document, need not be discussed. It has been admitted that basic algorithms already exist at least for routine products (*e.g.*, see SeaBAM Algorithm Evaluation, John E. O'Reilly and Stéphane Maritorena, NOAA, NASA, personal communication, 1997), and that algorithms for advanced products are still under development, although less essential for global monitoring.

At the beginning of the meeting in Villefranche-sur-Mer on the 6th October, 1997, it was realized and stated that the aim of the workshop was not to establish an "ideal" sensor, but to rely on the current state of knowledge, and on well-tried and accepted methodologies, so that one could progress by successive consensus towards the identification of "minimal" requirements for future ocean-colour instruments. In the same vein, the opinions expressed hereafter are those of the authors; in no way do they represent the policy of Agencies. The authors are the members of a working group set up by the IOCCG for addressing the questions outlined above. The membership of the working group is

- André Morel, Chairman
- Vittorio Barale
- Annick Bricaud
- Janet Campbell
- Nicolas Hoepffner
- Motoaki Kishino
- Marlon Lewis
- Shubha Sathyendranath
- James Yoder

Howard Gordon has been involved in reviewing successive drafts, and other information and help was provided by David Antoine, Paul Bissett, Chris Brown, Curtiss Davis, Mark Dowell, Wayne Esaias, Frank Mueller-Karger, and Venetia Stuart.The various Space Agencies with IOCCG representation were asked to provide the information presented in this document, and in particular, the information for the tables and appendices. The members of the working group apologise for any inadvertent omissions or inaccuracies.

# 2. Inventory of ocean-colour sensors (past, present, future); spectral bands, bandpass, noise equivalent radiances

This section provides basic information for past and present ocean-colour sensors (Table 1a), and for future sensors (Table 1b). The spectral bands of each of these sensors, together with their nominal bandwidths and noise equivalent radiances are summarized in Table 2. The band positions can be visualized in Appendix I. Note that the bands (in Tables and Figures) are only those dedicated to ocean-colour observation and associated atmospheric correction. Most of the future instruments also include other channels for other purposes (*e.g.* oxygen bands, vegetation, water vapor), not considered here.

More detailed information on the radiometric characteristics of the various sensors, and the way of deriving them, are provided in Appendix II.

**Table 1a. Characteristics of past and present ocean-colour sensors.**

| Sensor | CZCS | OCTS | POLDER | MOS | SeaWiFS |
|---|---|---|---|---|---|
| Platform | Nimbus-7 | ADEOS-1 | ADEOS-1 | IRS-P3 | OrbView-2 |
| Agency | NASA | NASDA | CNES | DLR | OSC/NASA |
| Country | USA | Japan | France | Germany/India | USA |
| Operation Start | Oct. 1978 | Aug. 1996 | Aug. 1996 | Mar. 1996 | Sep. 1997 |
| Operation End | Jun. 1986 | Jun. 1997 | Jun. 1997 | Mar. 2001 | Sep. 2002 |
| Orbital Inclination | 99.3 | 98.6 | 98.6 | 98.7 | 98.2 |
| Equatorial Crossing Time (h) | 12:00 | 10:41 | 10:41 | 10:30 | 12:00 |
| Altitude (km) | 955 | 804.6 | 804.6 | 817 | 705 |
| Resolution at Nadir (km) | 0.825 | 0.7 | 6 x 7 | 0.5 | 1.1 |
| Swath (km) | 1566 | 1400 | 2400 | 200 | 2800 |
| Tilt (degrees) | ±20 | ±20 | Variable | No | ±20 |
| Direct Link | No | UHF/X-band | X-band | S-band | L-band |
| Recorded | Yes | X-band | X-band | None | S-band |
| Solar Calibration | No | Yes | No | Yes | Yes |
| Lunar Calibration | No | No | No | No | Yes |
| Lamp Calibration | Yes | Yes | No | Yes | No |

**Table 1b. Characteristics of future ocean-colour sensors.**

| Sensor | OCM | MODIS-AM | MISR | OCI | OSMI | MERIS | GLI | POLDER-2 | MODIS-PM |
|---|---|---|---|---|---|---|---|---|---|
| Platform | IRS-P4 | EOS-AM1 | EOS-AM1 | ROCSAT | KOMPSAT | Envisat | ADEOS-2 | ADEOS-2 | EOS-PM1 |
| Agency | ISRO | NASA | NASA | Taiwan | KARI | ESA | NASDA | CNES | NASA |
| Country | India | USA | USA | Taiwan | Korea | Europe | Japan | France | USA |
| Operation Start | Nov. 1998 | 1999 | 1999 | Feb. 1999 | Jul. 1999 | Mar. 2000 | Jun. 2000 | Jun. 2000 | Dec. 2000 |
| Operation End | Nov. 2003 | Jun. 2003 | Jun. 2003 | Feb. 2003 | Jul. 2002 | Feb. 2004 | Jun. 2005 | Jun. 2005 | Dec. 2005 |
| Orbital Inclination | 98.3 | 98.2 | 98.2 | 35 | 98.13 | 98.5 | 98.6 | 98.6 | 98.2 |
| Eq. Crossing Time (h) | 12:00 | 10:30 | 10:30 | 09:00/15:00 | 10:50 | 10:00 | 10:30 | 10:30 | 13:30 |
| Altitude (km) | 720 | 705 | 705 | 600 | 685 | 800 | 803 | 803 | 705 |
| Resolution at Nadir (km) | 0.36 | 1 | 0.25 | 0.8 | 0.85 | 1.2/0.3 | 1/0.25 | 6 x 7 | 1 |
| Swath (km) | 1420 | 2330 | 360 | 704 | 800 | 1150 | 1600 | 2400 | 2330 |
| Tilt (degrees) | ± 20 | No | Variable | No | No | No | ±20 | Variable | No |
| Direct Link | X-band | X-band | No | S-band | X-Band | X-band | UHF/X-band | X-band | X-band |
| Recorded | Yes | X-band | X-band | None | Yes | X-band | X-band | X-band | X-band |
| Solar Calibration | Yes | Yes | No | — | Yes | Yes | Yes | No | Yes |
| Lunar Calibration | No | Yes | Yes | — | No | No | No | No | Yes |
| Lamp Calibration | Yes | Yes | No | — | No | No | Yes | No | Yes |

**Table 2. Summary of the spectral bands used for ocean-colour applications (see Appendix for detailed characteristics of these sensors).**
**Center λ (nm), Bandpass (FWHM, nm), NEΔL (W $m^{-2}$ $sr^{-1}$ $\mu m^{-1}$)**

**CZCS**

| Center λ | FWHM | NEΔL |
|---|---|---|
| 443 | 20 | 0.208 |
| 520 | 20 | 0.173 |
| 550 | 20 | 0.166 |
| 670 | 20 | 0.094 |
| 750 | 100 | 0.040 |

**OCTS**

| Center λ | FWHM | NEΔL |
|---|---|---|
| 412 | 20 | 0.186 |
| 443 | 20 | 0.109 |
| 490 | 20 | 0.089 |
| 520 | 20 | 0.121 |
| 565 | 20 | 0.091 |
| 670 | 20 | 0.037 |
| 765 | 40 | 0.057 |
| 865 | 40 | 0.031 |

**POLDER**

| Center λ | FWHM | NEΔL |
|---|---|---|
| 443 | 20 | 0.138 |
| 490 | 20 | 0.147 |
| 565 | 20 | 0.088 |
| 670 | 20 | 0.063 |
| 763 | 10 | 0.090 |
| 765 | 40 | 0.086 |
| 865 | 40 | 0.034 |
| 910 | 20 | 0.045 |

**MOS**

| Center λ | FWHM | NEΔL |
|---|---|---|
| 408 | 10 | 0.192 |
| 443 | 10 | 0.124 |
| 485 | 10 | 0.148 |
| 520 | 10 | 0.141 |
| 570 | 10 | 0.150 |
| 615 | 10 | 0.105 |
| 650 | 10 | 0.141 |
| 685 | 10 | 0.088 |
| 750 | 10 | 0.102 |
| 815 | 10 | 0.034 |
| 870 | 10 | 0.033 |

**SeaWiFS**

| Center λ | FWHM | NEΔL |
|---|---|---|
| 412 | 20 | 0.092 |
| 443 | 20 | 0.077 |
| 490 | 20 | 0.056 |
| 510 | 20 | 0.049 |
| 555 | 20 | 0.043 |
| 670 | 20 | 0.031 |
| 765 | 40 | 0.019 |
| 865 | 40 | 0.015 |

**MISR**

| Center λ | FWHM | NEΔL |
|---|---|---|
| 446 | 41 | 0.063 |
| 557 | 27 | 0.061 |
| 672 | 20 | 0.050 |
| 867 | 39 | 0.031 |

**MODIS**

| Center λ | FWHM | NEΔL |
|---|---|---|
| 412 | 15 | 0.048 |
| 443 | 10 | 0.032 |
| 488 | 10 | 0.025 |
| 531 | 10 | 0.018 |
| 551 | 10 | 0.019 |
| 667 | 10 | 0.008 |
| 678 | 10 | 0.007 |
| 748 | 10 | 0.009 |
| 870 | 15 | 0.006 |
| 469 * | 20 | 0.145 |
| 555 * | 20 | 0.127 |
| 645 ** | 50 | 0.170 |
| 858 ** | 35 | 0.123 |

**MERIS**

| Center λ | FWHM | NEΔL |
|---|---|---|
| 412.5 | 10 | 0.026 |
| 442.5 | 10 | 0.025 |
| 490 | 10 | 0.022 |
| 510 | 10 | 0.019 |
| 560 | 10 | 0.016 |
| 620 | 10 | 0.014 |
| 665 | 10 | 0.013 |
| 681 | 7.5 | 0.014 |
| 709 | 9 | 0.011 |
| 779 | 14 | 0.008 |
| 870 | 20 | 0.007 |
| 890 | 10 | 0.011 |
| 900 | 10 | 0.010 |

**OCI**

| Center λ | FWHM | NEΔL |
|---|---|---|
| 443 | 20 | — |
| 490 | 20 | — |
| 510 | 20 | — |
| 555 | 20 | — |
| 670 | 20 | — |
| 865 | 40 | — |

**OSMI**

| Center λ | FWHM | NEΔL |
|---|---|---|
| 443 | 20 | — |
| 490 | 20 | — |
| 510 | 20 | — |
| 555 | 20 | — |
| 670 | 20 | — |
| 865 | 40 | — |

**GLI**

| Center λ | FWHM | NEΔL |
|---|---|---|
| 380 | 10 | 0.076 |
| 400 | 10 | 0.051 |
| 412 | 10 | 0.045 |
| 443 | 10 | 0.054 |
| 460 | 10 | 0.055 |
| 490 | 10 | 0.027 |
| 520 | 10 | 0.044 |
| 545 | 10 | 0.044 |
| 565 | 10 | 0.018 |
| 625 | 10 | 0.017 |
| 666 | 10 | 0.015 |
| 680 | 10 | 0.014 |
| 710 | 10 | 0.012 |
| 749 | 10 | 0.010 |
| 865 | 20 | 0.007 |

**OCM**

| Center λ | FWHM | NEΔL |
|---|---|---|
| 412 | 20 | 0.26 |
| 443 | 20 | 0.22 |
| 490 | 20 | 0.17 |
| 510 | 20 | 0.17 |
| 555 | 20 | 0.15 |
| 670 | 20 | 0.10 |
| 765 | 40 | 0.05 |
| 865 | 40 | 0.08 |

**POLDER-2**

| Center λ | FWHM | NEΔL |
|---|---|---|
| 443 | 20 | 0.138 |
| 490 | 20 | 0.147 |
| 565 | 20 | 0.088 |
| 670 | 20 | 0.063 |
| 763 | 10 | 0.090 |
| 765 | 40 | 0.086 |
| 865 | 40 | 0.034 |
| 910 | 20 | 0.045 |

**S-GLI**

| Center λ | FWHM | NEΔL |
|---|---|---|
| 412 | 10 | 0.081 |
| 443 | 10 | 0.067 |
| 490 | 10 | 0.054 |
| 520 | 20 | 0.052 |
| 565 | 20 | 0.029 |
| 625 | 20 | 0.021 |
| 680 | 20 | 0.012 |
| 710 | 20 | 0.007 |
| 749 | 20 | 0.009 |
| 865 | 20 | 0.006 |

* Spatial resolution 0.5 km
** Spatial resolution 0.25 km
(others: 1km)

# 3. Scientific background: Ocean spectral reflectance interpretation, information *versus* number of channels

A general overview of this problem is given under the assumption that the atmospheric correction is "perfectly" made. The constraints imposed by the need for an accurate atmospheric correction, combined with those of deriving a useful ocean-colour signal are examined in section 4.

## 3.1 Information content and spectral resolution

Until 1996, all our practical experience of satellite ocean-colour techniques came from a single, experimental, satellite sensor: the Coastal Zone Colour Scanner (CZCS), launched by NASA in late 1978, and operated until the first half of 1986. New and improved ocean-colour sensors have recently been launched by Japan, France, Indo-Germany and the USA, but the potentials of these new experiments are still being explored. Various countries plan even more sophisticated satellite sensors for the next few years (see Table 1b). The CZCS had very modest spectral resolution and a modest goal of estimating a phytoplankton pigment index, whereas the new generation of present and future satellite sensors have improved spectral resolution, aimed at retrieving more information from ocean colour, or at improving the accuracy and precision of retrievals of pigment concentration. The success of these more ambitious goals still remains to be evaluated.

In such a context, it is difficult, if not impossible, either to draw solely on practical satellite experience to evaluate the information content in the ocean-colour signal, or to discuss the choice of wavelengths for ocean-colour missions. Instead, in this section, we shall base our discussions on theoretical grounds, on results of optical *in situ* determinations, and on practical experiences of remote sensing from aircraft. For the conclusions drawn from such analyses to be valid in the context of satellite remote sensing, the atmospheric correction has to be implemented "perfectly" (see section 4). With this *proviso*, we give, in this section, a general overview of the potentials and problems of remote sensing of ocean colour.

In the theoretical discussions, we recognize that ocean colour, or spectrally-resolved reflectance at the sea surface, is generally modeled as simple functions of the absorption coefficient and the back-scattering coefficient of the water body (*e.g.*, Gordon *et al.*, 1975; Morel and Prieur, 1977; Kirk, 1981; Åas, 1987; Sathyendranath and Platt, 1997), with additional influence from inelastic processes such as Raman scattering (Sugihara *et al.*, 1984), fluorescence by chlorophyll-*a* (Neville and Gower, 1977; Morel and Prieur, 1977; Gordon, 1979), and fluorescence by organic dissolved materials (Hawes *et al.*, 1992; Lee *et al.*, 1994). We also recognize that phytoplankton pigments influence ocean colour for the most part through their influence on the absorption spectrum, except when fluorescence by chlorophyll-*a* (around 685 nm), or by biliproteins (Yentsch and Phinney, 1985) alters significantly the signal in specific wavebands. The reflectance spectra of oceanic (Case 1) waters could be split into two spectral regions (see *e.g.* Haltrin *et al.*, 1997): a blue part ($\lambda < 590$ nm) notably affected by elastic-scattering effects, and a red part (> 590 nm) notably affected by inelastic processes. Red fluorescence near 685 nm, caused by chlorophyll, plays a dominant role when the algal concentration is large, whereas in oligotrophic and mesotrophic waters, Raman emission is the main inelastic process, which actually affects the whole spectrum (Stavn, 1990, 1992). For those Case 2 waters where the dissolved organic matter is abundant (yellow-substance-dominated Case 2 waters), the blue fluorescence by this coloured substance may become an important contributor to the reflectance (Hawes *et al.*, 1992; Haltrin *et al.*, 1997; Dowell and Hoepffner, 1997). With this background, we can explore the usefulness of wavelengths in a remote-sensing context.

## 3.2 Phytoplankton pigments and their influence on absorption and reflectance spectra

As a first step in identifying the wavelengths that carry useful information in an ocean-colour, remote-sensing context, we can examine the relationship between phytoplankton pigments and their absorption spectra. At an elementary level, it may be argued that the single most important phytoplankton pigment is chlorophyll-*a*, and that, if we are only interested in retrieving that one variable, then it should be possible to achieve the goal if we know phytoplankton absorption at one suitable wavelength. To a large extent, such an approach is feasible, for Case 1 waters, in particular. In fact, simple optical models for such open ocean waters rely on the observation that it is possible to parameterize entire, spectrally-resolved, optical properties of the water body if we know the concentration of chlorophyll-*a* in the water (Gordon *et al*., 1988; Morel, 1988). Bricaud *et al.* (1995) have recently shown that the phytoplankton absorption at every single wavelength in the visible domain can be parameterized as a function of the chlorophyll-*a* concentration (see also Cleveland, 1995). Implicit in such parameterizations is the assumption that the pigment composition of algae evolves in a regular (and predictable) way from oligotrophic to mesotrophic, and eutrophic Case 1 waters.

However, in such parameterizations, there is always a considerable amount of unexplained variability, and at the next level of complexity we can ask whether the residual variability carries any useful information. One potential source of this variability is fluctuations in the concentrations of auxiliary pigments relative to that of chlorophyll-*a*. From classical plant physiology, we know that the exact composition of phytoplankton pigments varies with changes in the phytoplankton species composition, or in the physiological state of a given phytoplankton species. In recent years, several studies have shown that some variability in the shapes of phytoplankton absorption spectra is related to changes in the packaging effect (Morel and Bricaud, 1981; Roesler *et al.*, 1989; Sosik *et al.*, 1989), as well as in the pigment composition (Mitchell and Kiefer., 1988; Bricaud and Stramski, 1990; Hoepffner and Sathyendranath, 1992). The inverse problem of retrieval of pigment composition from absorption spectra is not trivial, for various reasons: a large number of phytoplankton pigments are present in natural phytoplankton populations (a typical High Performance Liquid Chromatography analysis would probe a phytoplankton sample for some 15 pigments and their degradation products, not including biliproteins); the absorption bands of individual pigments overlap each other; and variations in pigment packaging in phytoplankton cells can influence their absorption efficiencies.

However, promising techniques exist for recovering some pigment information from absorption spectra (Bidigare *et al.*, 1989). Hoepffner and Sathyendranath (1991, 1993), for example, have developed a technique that has the potential to decompose individual absorption spectra into about a dozen or so Gaussian bands associated with chlorophylls-*a*, *b*, and *c*, and carotenoids. Such analyses suggest that some information on phytoplankton pigment composition may be retrievable, provided that data on absorption are available at ten or so wavelengths, selected to match the absorption maxima of these individual pigments.

Thus, the goal of retrieving some information on pigment composition rather than just on the main pigment, chlorophyll-*a*, increases the wavelength requirement by an order of magnitude. New results (Sathyendranath, unpublished results) also suggest that small changes in the position of the Gaussian bands, or in their bandwidths, may be associated with yet more changes in pigment composition, such as changes in divinyl-chlorophyll-*a* relative to normal chlorophyll-*a*, when the phytoplanktonic assemblage includes prochlorophytes (Chisholm *et al.*, 1988; Morel *et al.*, 1993). But obtaining information on band widths of individual Gaussian bands or on small changes (1~3 nm) in the band positions requires that we have absorption spectra resolved to about one nm, within the spectral domain of 400-700 nm, thus increasing the resolution requirement by another order of magnitude.

Another point to bear in mind when discussing the retrieval of algal concentration in the near surface layer is that a possibility exists for passive remote sensing of chlorophyll-*a*, through the sun-induced fluorescence signal (Neville and Gower, 1977; Gower and Borstad, 1981). Even though the effectiveness of such a method has not been demonstrated using satellite data, there is every evidence that this technique could be useful in Case 2 waters, and even in oceanic Case 1 waters with moderate chlorophyll concentrations (Babin *et al.*, 1996). The MODIS and MERIS instruments are designed for such an application (Letelier and Abbott, 1996). Besides a low noise-equivalent radiance, the fluorescence detection requires additional channels in the red part of the spectrum; at least three dedicated channels are necessary to monitor the height of the fluorescence signal above a baseline determined using two channels on either side of the emission peak.

Up to this point, we have discussed the information content in only the optical properties of phytoplankton. When dealing with reflectance spectra of natural sea water samples, additional issues have to be addressed: in particular, the high absorption coefficient of the water itself at wavelengths larger than about 590 nm overwhelms the absorption signatures of other substances. In addition, reflectances are governed by the spectral dependency both of absorption and of backscattering. Even in Case 1 waters, where most of the suspended materials often originate from biological activity, the spectral dependency and the magnitude of the backscattering coefficients are not fully understood (nor predictable). As a result, reflectance spectra are non-linear functions of absorption, and strong signals in absorption may be reduced to a small signal in reflectance. Thus, the problem of retrieving pigment information from optical data is more complicated for sea surface reflectance than for phytoplankton absorption spectra.

But Gege (1997) has analyzed high-resolution (512 channels in the 400-800 nm range) reflectance spectra measured from a boat on Lake Constance, and shown that these spectra can be used to quantify the concentrations of four phytoplankton species that are known to occur at high abundances in the lake. His analysis is based on exploiting the differences in the absorption spectra of these phytoplankton species, which in turn are related to differences in their pigment compositions. Information on spectral absorption or reflectance properties of unusual algal blooms, such as coccolithophores (Viollier and Sturm, 1984; Gordon *et al.*, 1988; Ackelson *et al.*, 1994; Balch *et al.*, 1996), *Trichodesmium* (Subramaniam and Carpenter, 1994), and *Mesodinium rubrum* (Doerffer, unpublished data) also show that some bloom-forming algae have spectral signatures that are very distinct from the more-commonly-encountered phytoplankton communities, again suggesting that it may be possible to identify such blooms from remotely-sensed data.

In fact, methods already exist for identifying coccolithophore or *Trichodesmium* blooms using CZCS data (Brown and Yoder, 1994; Subramaniam and Carpenter, 1994), though quantifying the pigment concentrations within the blooms remains more problematic. These results are encouraging (but see Garver *et al.*, 1994); at least under some favorable conditions, they support the idea that additional information on pigment composition or on species composition of phytoplankton can be recovered from reflectance spectra, provided high-resolution spectral information is available.

## 3.3 The need for additional wavelengths

Up to now, we have considered mainly how the wavelength requirements increase when we explore the possibility of retrieving, in Case 1 waters, more than one pigment index from ocean-colour data. In coastal Case 2 waters, the influence of other substances, such as dissolved organic (coloured) matter and of suspended sediments may be very important, and may vary independently of the chlorophyll concentration. Dissolved coloured substances affect only the absorption coefficient, whereas suspended minerals may strongly enhance the scattering coefficient, with a minor, albeit non-negligible, impact on absorption. Similar arguments as above for Case 1 waters can be made for application of ocean-colour data in these more complex waters, where the need for additional wavelengths emerges from the requirement to separate the various dissolved and particulate materials. In this context also, it quickly becomes apparent that the possibility of retrieval often increases with increasing spectral resolution.

The goal here is to identify and, ideally, quantify three variables: a phytoplankton pigment “index”, concentration of dissolved organic matter and concentration of suspended sediments. So it may be argued that the problem should be solvable if we had information on ocean colour at three suitable wavelengths, and if we could rely on stable optical (specific absorption and backscattering) coefficients for the three components. But typically, addressing the problem with some degree of confidence requires information at more than three wavelengths. This requirement arises from a number of factors:

- The spectral features of interest are broad, they overlap each other, and, in certain spectral windows, they resemble each other.
- No single wavelength can be treated as a unique signal carrier for any of the components of interest.

- The relationships between ocean colour and optical properties of the component of interest are non-linear.

Under these circumstances, sophisticated optimization techniques are envisaged to solve the problem. When such techniques are used in a context where the data are not error-free, redundancy is often essential to constrain the solutions.

## 3.4 Do the same wavelengths always carry the same information?

The oceans are complex and diverse, and it is possible that wavelengths often used as signal carriers for a given variable may become contaminated by the influence of other variables, such that the interpretation of the signal at those wavelengths becomes difficult. For example, in the time-honored algorithm for retrieval of a phytoplankton pigment index, changes in the blue-green ratio of reflectance are interpreted as changes in chlorophyll-*a*.

However, we know that substances other than chlorophyll-*a* can change the blue-green ratio. Most important of these is dissolved organic matter or yellow substance, which has a strong influence on the blue-green ratio. In Case 2 waters with large quantities of yellow substances, it would be impossible to distinguish them from phytoplankton pigments, if the blue-green-ratio algorithm were used (Fischer *et al.*, 1986).

Changes in species composition can also modify the blue-green ratio without any change in the concentration of chlorophyll-*a*. For example, variations in the proportion of fucoxanthin relative to chlorophyll-*a* can change the blue-green ratio of phytoplankton absorption by a factor of up to six (Hoepffner and Sathyendranath 1992). Morel (1997) has shown that the blue-green ratio of waters dominated by a *Synechococcus* bloom may be different from that of waters with a "normal" phytoplankton population having the same amount of chlorophyll-*a*. Such a difference may overestimate chlorophyll-*a* values by as much as a factor of three, if routine algorithms are used. It therefore becomes essential to use additional wavelengths to identify such special situations and, if possible, apply correction factors.

Thus, high spectral resolution in ocean-colour data is desirable, not just in the context of retrieving additional information from ocean colour, but also in the context of making the estimates of pigment index more rigorous and robust. If the number of channels is deliberately reduced (see section 4), it must be accepted that some uncertainties and ambiguities will remain in routine estimates.

## 3.5 Problem solving in a high-noise environment

It is important to point out here that the usefulness of multiple wavelengths in a remote-sensing context is linked to the precision in the data. Many of the more advanced applications, such as deriving information on pigment composition, rely on retrieving signals of very small magnitudes, and so the usefulness of multiple wavelengths is likely to be compromised if the ocean-colour information is not available at the necessary precision and accuracy. For example, Fischer (1985) has shown that, for a given number of wavelengths, the number of independent pieces of information that can be retrieved will drastically decrease with increasing noise in the data. Thus, to meet the more demanding requirements of ocean-colour missions, the increased spectral resolution of the sensors must be matched by increased precision in the retrieved ocean-colour signal, which in turn demands improvements in both instrument design and atmospheric correction techniques.

All these analyses show that the wavelength resolution required, and the precision needed in the retrieval of ocean colour, are linked to the objectives of the remote-sensing experiment. The more ambitious goals, and the more stringent requirements, can be met only through very high spectral resolution, and very high precision in the retrieval of ocean-colour spectra. Any choice of a small number of wavelengths for a satellite mission must therefore be recognized as a compromise, and it would be unreasonable to expect that any subset of potentially useful bands would meet all contingencies.

## 3.6 Loss of information when wavelengths are dropped

In the preceding sections we saw how the number of wavelengths required in a remote-sensing study increased as the goals become more demanding. Conversely, we can explore whether full spectral information is always needed, or whether wavelengths can be dropped while retaining all useful information contained in high-resolution data. This complex problem can be studied only in specific contexts. The technique that has been followed with some success involves starting with high-resolution spectral information, and evaluating the information content in the data set. Then, wavelengths are dropped successively from the data set, and the change in retrieved information, if any, is evaluated. The quality of the technique used for information retrieval can be evaluated on the basis of the tightness of the relationship between the ocean-colour signal (if necessary after some transformations) and an oceanic property of interest; on the basis of the stability of the relationship when perturbations are introduced; or on the basis of the linearity of the relationship.

Principal component analysis has been used in some studies to address this problem. Sathyendranath *et al.* (1989) examined the retrieval, in case 2 waters, of three optically active components, namely algal pigments, suspended material and dissolved organic matter (see also Dowell and Hoepffner, 1997). The choice of wavelengths to retain can be based on a number of criteria. If, in certain spectral domains, the characteristic spectra of the variables are similar to each other, we can then conclude that those spectral domains cannot be used to distinguish between the variables of interest. The corresponding bands may be dropped from the sensor without loss of information. Conversely, we could select those wavebands in which the characteristic spectra of the individual variables appeared to be most different from each other. Or, one could examine the correlation between wavelengths, and if two wavelengths were perfectly correlated, one of them could be dropped. Sathyendranath *et al.* (1989) concluded that one could reduce the number of wavelengths from 30 to 5, without significant loss of information, provided the wavelengths retained were selected judiciously. By using a five-band approach, it has been shown that a full spectrum reconstruction would be possible (Wernand *et al.*, 1997). In a similar study, Sathyendranath *et al.* (1994) examined the wavelength requirements for distinguishing chlorophyll-*a* from phycoerythrin (a biliprotein), and again found that the task could be accomplished successfully using five wavelengths, whereas using only three wavelengths led to a significant decrease in the performance.

In interpreting the results from these analyses, it is also important to recognize the limitations of the techniques used. The problem is inherently non-linear, and principal component analysis is a linear technique. The approach is a purely statistical one, and gives no indication of how the results might be extrapolated to other situations. The analyses may use observations or modeled reflectance spectra as inputs, and the results will be compromised if the inputs are not sufficiently representative. Within these limitations, the studies cited above suggest that, if the goal is to estimate two or three independent variables from ocean-colour data, then we need at least five wavebands, whereas three CZCS-type wavebands may be insufficient for the task. This guideline will be used in the next section.

# 4. Practical aspects: Number of channels *versus* objectives

## 4.1 Atmospheric correction requirement

Before any interpretation of the marine signals can be made, the crucial problem in detecting ocean colour from space is to make an accurate "atmospheric correction". As is well known, backscattered radiation by air molecules and aerosols is predominant (80% or more) in forming the radiance detected at the top of the atmosphere (TOA) in the visible part of the spectrum. The aerosol nature and optical thickness are additional unknowns in the ocean-colour remote sensing problem. Whatever the technique employed for removing the atmospheric contribution (not discussed here), specific information about aerosols is needed. This information is available in the near infrared part of the spectrum (NIR), where the atmospheric contribution to the TOA radiance becomes 100%, to the extent that the marine signal, at least for case 1 waters, vanishes in this spectral domain. Because aerosol scattering varies spectrally, and presumably in a smooth manner, at least two measurements at two wavelengths are necessary and thus represent a minimal requirement. These two wavelengths, or channels, must be sufficiently distant from each other in the NIR to capture the spectral trend with some accuracy; in addition, they must be not too far from the visible domain, to ensure a safe extrapolation toward this domain. The last consideration when making the NIR channel selection is to avoid prominent atmospheric absorption bands (water vapor and oxygen), which exist in this spectral domain. Safe and "clear" windows, with sufficient width (reference HITRAN, Rothman *et al.*, 1987, 1992), are as follows:

| | | | | | |
|---|---|---|---|---|---|
| (0) Between | 1024 | and | 1064 nm, | transmittance above 0.998 |
| (1) Between | 855 | and | 890 nm, | transmittance above 0.998 |
| (2) Between | 772 | and | 786 nm, | transmittance above 0.998 |
| (3) Between | 744 | and | 757 nm, | transmittance above 0.995 |
| (4) Between | 704 | and | 713 nm, | transmittance above 0.978 * |

* for 2 cm precipitable water

The adoption of channel (1), actually used for almost all instruments, is obviously a good choice. The available width of this atmospheric window and thus of the bandpass, can warrant a favorable S/N ratio; in addition, this wavelength is far enough away from the visible range, therefore a good assessment of the spectral scattering behaviour can be achieved.

A combination of channel (1) and channel (3) seems the most favorable. Indeed, channel (4), closer to the visible domain, and farther from (1), could appear even more convenient than channel (3). Information in this channel, however, is occasionally contaminated by a residual marine signal, in very high chlorophyll waters, or in transition zones between Case 1 and turbid-Case 2 waters. Therefore channel (3) is safer than channel (4) from this point of view, and is wider.

A combination of channels (1) and (2) (instead of (3)), was adopted for MERIS. Such a choice originates from a compromise with another mission of MERIS, namely the detection of the cloud top height. This detection requires a narrow reference band (no oxygen absorption), close to the oxygen absorption band (at $\lambda$ = 760 nm); this reference band was located around 754 nm. As a consequence, the position corresponding to channel (3) is no longer available for atmospheric correction, whence the resort to the channel (2) in combination with (1) for the MERIS instrument.

Using two channels, as (1) and (3), may result in significant errors in the atmospheric correction, in presence of whitecaps (Frouin *et al.*, 1996; Gordon, 1997); the addition of channel (0) has been proposed to reduce the errors, by exploiting differences in the spectral properties of aerosol scattering and whitecap reflectance in this NIR domain.

As a preliminary conclusion, a *minimum minimorum* set could be the couple (1) and (3). If flexibility exists, adding channels (4) and/or (0) could offer advantages. In most situations, with no appreciable marine signal, the extrapolation toward the visible domain can be made more robust if channel (4) is available. Possibly, an additional piece of information could also be extracted from this channel concerning the detection of absorbing aerosols, when present. The problem of whitecaps could lead to a recommendation for the further adoption of channel (0).

## 4.2 Pigment index (chlorophyll) retrieval

The "colour" of oceanic Case 1 waters shifts from deep blue in oligotrophic waters (very low chlorophyll concentration) to dark green in eutrophic waters (high concentration). This shift results from the strong absorption by algal pigments (not only chlorophyll, but also various carotenoids) in the blue band, with a maximum around 445 nm, compared with the weak absorption in the green-yellow band (550-580 nm). The reflectances, $R$, for these two bands, or the normalized water-leaving radiances, $(L_w)_N$, are combined through their ratio. The rationale for using a ratio technique, rather than another kind of combination (a difference, for instance), lies in the variability and the uncertainty affecting the absolute values of $R$ or $(L_w)_N$. Natural as well as methodological sources of variations and errors inevitably interfere. The quantities $R$ and $(L_w)_N$ are directly sensitive to the scattering and backscattering coefficients, in such a way that they may vary by a factor 2 or more, for a given chlorophyll con-centration, whereas spectral ratios remain practically unaffected. Also, the impact of the bidirectional character of the ocean reflectance is greatly reduced if a ratio is used. After the atmospheric correction process, residual errors may persist and are added to the marine signals at the two wavelengths. Their impact is considerably diminished for the ratio.

As an obvious preliminary conclusion, a couple of wavelengths constitutes the *minimum minimorum*. The position of the needed channel in the green region of minimal absorption is constrained by the existence of an atmospheric absorption band (due to water vapor, from 567 to 637 nm). Therefore, depending on the bandwidth, the wavelengths 555 nm (20 nm wide), or 560 nm (10 nm wide) are convenient. The other mandatory channel must be located within the blue absorption band of algae. Ideally, the most appropriate channel corresponds to the phytoplankton absorption maximum, occurring on average at about 443 nm. Indeed, the ratio $R(443)/R(555)$ spans a wide range, and may vary from about 10, down to 0.3, when chlorophyll varies from 0.02 to 20 mg m$^{-3}$. An objection has been raised against this blue wavelength, because of its great distance from the NIR channels, rendering the extrapolation, and thus the atmospheric correction, somewhat problematic. Another objection was the vanishingly small marine signal at 443 nm, for pigment concentrations above 2 mg m$^{-3}$.

An alternative solution has been proposed (*e.g.*, see the presently used SeaWiFS algorithms), in which the above ratio is replaced by the ratio $R(490)/R(555)$.

It is, however, notably less sensitive, as it varies from about 5 down to 0.5 for the same chlorophyll concentration range as envisaged above. It is nevertheless believed that this disadvantage would be compensated by the better accuracy of the atmospheric correction at the wavelength 490 nm, compared with that achievable at 443 nm, as well as by a more substantial marine signal at 490 nm, when the chlorophyll content becomes high. Admittedly, this question is still open and will remain so until experience is gained in the near future (particularly with the SeaWiFS sensor). Nevertheless, it can be noticed that in the range of low (say, <0.30 mg $m^{-3}$) chlorophyll concentration (typical of the open ocean), there is a definite advantage in using the first colour ratio, as it decreases by a factor of three when the chlorophyll concentration increases from 0.03 up to 0.3 mg $m^{-3}$, whereas the second ratio decreases only by a factor of 1.3 over the same concentration range. A switching procedure, from the first to the second ratio, has already been proposed, to be operated as soon as the signal at 443 nm becomes lower than that at 490 nm, and such a procedure seems very reasonable.

Therefore, at this stage, and with the principal aim of estimating the chlorophyll concentration in Case 1 waters, the conclusion could be i) to select the 490-560 nm couple, as a first priority, in conformity with previous choices, and ii) to advocate strongly for an additional capability, as provided by the adoption of the triplet 443-490-560 nm.

Experience of the past (CZCS), leads us to think that with this set of NIR and VIS channels, discriminating between Case 1 waters and turbid-Case 2 waters is feasible, by using a threshold technique applied to the marine signals, all enhanced in turbid waters (Bricaud and Morel, 1987). Based on the reflectance values, a rough estimate of the sediment load can be made at 555 nm, for instance. Nonetheless, a more accurate quantification of this load will necessarily require specific field studies, aiming at relating the mass concentration to the scattering properties of the local sediments. Some interferences seem inevitable; highly loaded waters exhibit a non-zero signal in the infrared domain and therefore may induce an overestimate of the aerosol contribution. The differing spectral behavior of the scattering by aerosols and by hydrosols could help in removing ambiguities; other techniques, based on the "bright pixel" (Moore *et al.*, personal communication, 1998) are under development.

Yellow-substance-dominated Case 2 waters cannot be detected with this minimal set of two or three wavelengths. Generally, they will be interpreted as being Case 1 waters, with rather high chlorophyll concentration. The divergence between the optical signatures of algae and of yellow substances takes place at shorter wavelengths, when phytoplankton absorption tends to decrease (between 440 and 380 nm), whereas yellow substance absorption continues to increase in an exponential fashion. Beside instrumental limitations, the extreme difficulty of performing atmospheric corrections in the near UV has led to the proposal of a "violet" channel at about 410 nm. Disposing of such a channel appears to be the unique solution to get information about yellow substances, at least for a simple instrument and with simple algorithms based on reflectance ratio techniques. In such a perspective, a comparison of ratios like $R(410)/R(555)$ and $R(443)/R(555)$(or other possible combinations as well) could provide a clue to identifying zones where yellow substances becomes the dominant optically active substance. It must be acknowledged that, if algorithms have been put forward tentatively for the detection and quantification of yellow substances, a convincing demonstration of their efficiency has not yet been made. This situation should improve rapidly, thanks to experience to be gained with the new sensors.

As soon as a combination of four visible channels (410, 443, 490, and 555 nm) can be accepted, even for a simple instrument, other approaches, more complex than simple ratio techniques, are potentially conceivable. Among them, non-linear inversion or neural network techniques could be employed. In principle, the capabilities of such advanced methods increase when the number of channels and spectral information increases, and thus when the problem becomes more constrained (see section 3). But, with more than 4 channels in the visible part of the spectrum, we would leave the domain of simple sensors, and enter that of sophisticated sensors, outside the scope of this work.

In summary, after having catalogued the channels as follows:

| | | | |
|---|---|---|---|
| # 0 | 1024 – 1064 nm | width | 30 nm (possible width 40 nm) |
| # 1 | 855 – 890 nm | width | 20 nm (possible width 35 nm) |
| # 2 | 744 – 757 nm | width | 14 nm |
| # 3 | 704 – 713 nm | width | 10 nm |
| # 4 | 550 – 565 nm | width | 10 nm |
| # 5 | 485 – 495 nm | width | 10 nm |
| # 6 | 438 – 448 nm | width | 10 nm |
| # 7 | 407 – 417 nm | width | 10 nm |

the following combinations (“C*n*”) can be envisaged:

| | |
|---|---|
| C1 = Channels | 1, 2, 4, 5 |
| C2 = Channels | 1, 2, 4, 5, 6 |
| C3 = Channels | 1, 2, 4, 5, 6, 7 |
| C4 = Channels | 1, 2, 3, 4, 5, 6 |
| C5 = Channels | 0, 1, 2, 4, 5, 6 |
| C6 = Channels | 1, 2, 3, 4, 5, 6, 7 |
| C7 = Channels | 0, 1, 2, 3, + *n* channels in the visible part of the spectrum |

with the following comments:

- The combination C1 (restricted to 4 channels) represents a *minimum minimorum* in terms of atmospheric correction and of ocean-colour information, providing a single pigment (“chlorophyll”) estimate within Case 1 waters, and a crude delineation of the turbid-Case 2 waters.
- The combination C2 (5 channels) provides a better assessment of the chlorophyll concentration over its whole range, including that of low to very low concentrations, and a safer discrimination of turbid waters, including a quantitative information about their reflectance.
- The combination C3 (6 channels) has the same capacity as C2, and, in addition, implementation of the specific channel centered on 412 nm can remove ambiguities between the effect of algal pigments and that of yellow substance; in addition, this channel can help in the detection of absorbing aerosols above open ocean.
- The combination C4, also with 6 channels, has the same capacity as C2, in terms of marine information, but the atmospheric correction could be improved thanks to the availability of three channels in the near infra-red domain, allowing more accurate products to be expected.
- The combination C5, again with 6 channels, differs from C4 only for the atmospheric correction procedure, and could offer a capacity in distinguishing between whitecaps and aerosols.
- The combination C6 (7 channels), combines the advantages of C3 and C4, namely an improved atmospheric correction and a yellow substance detection capability.

- The combination C7 (*n* >7 channels) represents any advanced, sophisticated sensor, with added capacities (*cf.* section 3), and thus falls outside the scope of the present document.

For the visible channels, the proposed 10 nm bandwidth is desirable to maximise the differences between channels 4 to 7, and to increase the potential for retrieving some information on algal pigment composition. Though it is acknowledged that retrieval of pigment composition by remote sensing has yet to be demonstrated irrefutably, bandwidths of 10 nm in the visible should nevertheless be seen as a desirable configuration for future sensors.

# 5. Other requirements

## 5.1 Radiometric calibration, solar calibration, vicarious calibration

As a prerequisite, ocean-colour applications need an accurate radiometric calibration of the sensor to reach the required accuracy of the remotely sensed signals. The CZCS experience, which was affected by severe malfunctioning of internal calibration and had to rely most of the time upon vicarious calibration, has drawn attention to the importance of setting up well-defined and reliable calibration procedures. The radiometric accuracy requirements set for SeaWiFS and MODIS, for instance, have been (for the visible range) 5% for absolute radiance values, and 2% for relative values (reflectances). These specifications must be met for the whole spectral range and the whole field-of-view of the sensor. These goals are usually reached by combining internal calibration procedures and vicarious calibration based on *in situ* measurements.

### *5.1.1 Internal calibration:*

To satisfy the high calibration standards mentioned above, the basic requirement is to make use of an on-board, in-flight calibration system. Generally, the new sensors rely on a solar diffuser plate viewing the sun (instead of internal calibration lamps, which proved to be unreliable for CZCS). Such a diffuser, illuminated by the sun, provides a calibration relative to the solar irradiance. Knowing the solar constant (and its slight variations with the solar cycle), it is then possible, under the assumption of the diffuser stability, to monitor a possible drift of the instrument. Solar observations are usually made over the Pole so as to minimize the loss of oceanic measurements, and can be as frequent as once per orbit.

Obviously, the reflectance and bidirectional properties of the solar diffuser have to be characterized precisely during the pre-launch phase using laboratory calibration devices. However, as this diffuser is permanently exposed to sunlight and UV radiation after launch, it is expected to degrade with time. It is therefore useful, as it is the case for SeaWiFS, to add an attenuator plate that attenuates the flux incident on the diffuser plate and limits its degradation. However, even in this case, it remains necessary to track the actual degradation of the solar plate.

The concept used for SeaWiFS and MODIS is to use the surface of the moon as a secondary diffuser, *i.e.*, to compare the sunlight scattered by the surface of the moon with that scattered by the solar diffuser. The basic assumption is that the surface of the moon is perfectly stable with time. However, the reflectance of this surface is not spatially homogeneous, so that the correction procedure must take into account these spatial variations and the observation geometry. With this aim, a database of radiometric observations of the moon has been developed for SeaWiFS. The frequency of lunar observations (once per month at the most for full illumination) must, in practice, be decided according to the rate of degradation of the solar diffuser.

In addition to the lunar observations, the MODIS instrument controls the behavior of the diffuser with an additional design, the "solar diffuser stability monitor". It consists of a spherical integrating source with nine filtered detectors, viewing, alternatively, direct sunlight and the illuminated solar diffuser, so that changes in the reflectance of the diffuser can be monitored at nine wavelengths between 0.4 µm and 1 µm. Another solution, developed for MERIS, is to use two diffuser plates mounted on a "calibration wheel", the first one permanently exposed to sun irradiance, whereas the secondary one, much less frequently exposed, is used to monitor the degradation of the primary diffuser. Whatever the system adopted, such monitoring remains critical to an accurate calibration of measured radiances.

### *5.1.2 Vicarious calibration:*

Vicarious calibrations consist of comparisons between water-leaving radiances at the sea level and those derived from satellite measurements, after proper atmospheric corrections. Such vicarious calibrations may be useful as additional tests to check the functioning of the sensor. The difficulty, however, lies in that not only the sensor calibration, but also the quality of atmospheric corrections, is tested using this approach. Therefore, vicarious calibration must be considered only as an additional check of the whole system (sensor + atmospheric algorithms) function, with the calibration of the sensor relying primarily upon the in-flight diffuser system. The analysis of differences between vicarious calibration and on-board calibration may be useful to determine the sources of errors.

Vicarious calibrations are usually performed in oceanic sites characterized by weak variability in optical properties, such as very oligotrophic waters. Even in such a case, spatial and temporal variations of water-leaving radiances have to be taken into account (particularly at 443 nm, where the variability of radiance is high at low chlorophyll content). To minimize errors in atmospheric corrections, atmospheric properties (*e.g.* optical thickness of aerosols, aerosol phase function, ozone content) have also to be determined accurately. Therefore, an extended set of *in situ* oceanic and atmospheric measurements must be performed at the time of the satellite overpass, in the same way as in "validation experiments" (see Mueller and Austin, 1995). Such measurements can be performed from ship. The CZCS experience, however, has shown that the monitoring of the system is more reliable if it is made at high frequency. Therefore it is useful to include in such experiments not only ship measurements, but also measurements from fixed optical moorings providing time-series for adequate parameters.

In conclusion, whatever the degree of simplification that is envisaged for a low-cost sensor, the high radiometric stability and control capabilities cannot be less than those anticipated for the future sophisticated sensors. In other words, there is no possible simplification or relaxation of constraints in this domain.

### *5.1.3 Noise Equivalent Radiance:*

The same conclusion holds true for the noise-equivalent-radiance in all channels, including those devoted to the atmospheric correction. Studies made in different agencies and scientific teams lead to specifications, actually very similar, as recommended for the next generation of sensors (see Figure 1), now achievable with modern technology. Even for simple sensors, such requirements, say NE$\Delta$L below 0.05, or better, below 0.035 W $m^{-2}$ $sr^{-1}$ $\mu m^{-1}$ in the visible and near infrared, and below 0.025 in the NIR, must be kept. Such noise-equivalent-radiance requirements, actually met by future instruments such as MODIS, MERIS and GLI, must be aimed at for less sophisticated instruments as well.

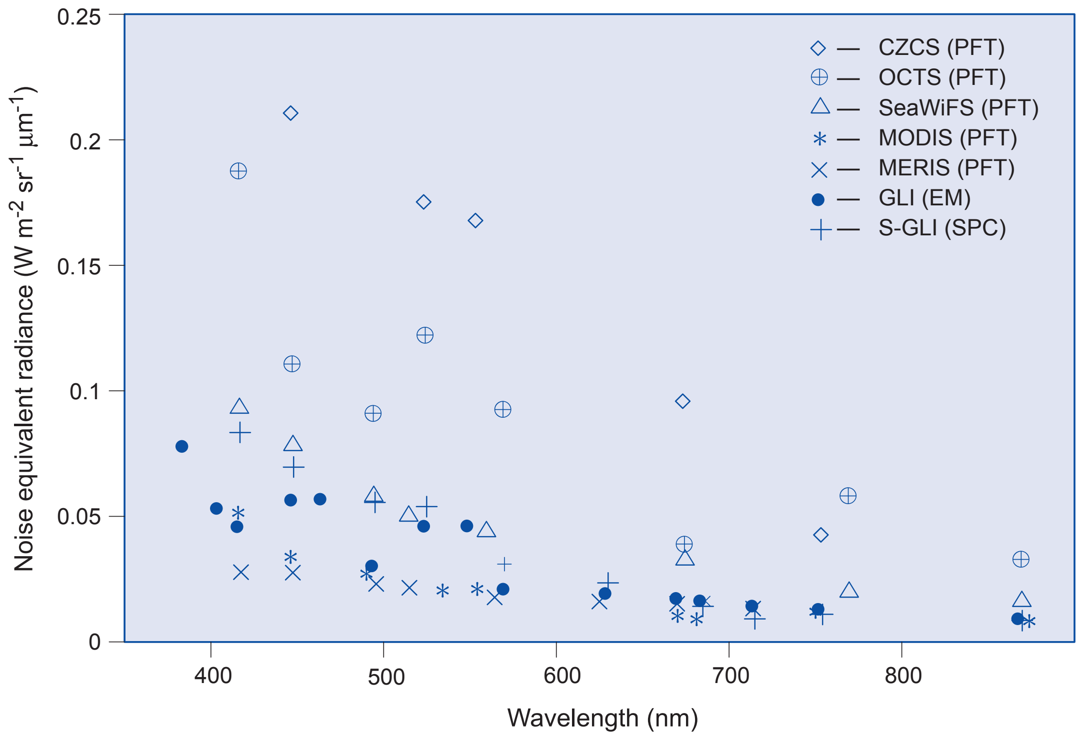


**Figure 1. Noise equivalent radiance of various satellite ocean-colour sensors**

## 5.2 Dynamic range

The dynamic range for each channel has to be adjusted in such a way that a maximal sensitivity is achieved when the sensor is pointed at the ocean. This requirement (optimization for dark targets) for ocean-colour observations can be a major factor in instrument design. One approach taken has been to allow the sensor to saturate over bright targets, such as clouds or possibly many terrestrial sites, and instead, to accommodate only radiances expected over cloudless ocean pixels. This precludes knowing how bright the brightest pixels were, if corrections are needed.

As aerosol optical thickness and nature constitute extremely valuable products, and are, in principle, determined as accurately as the atmospheric correction has been achieved, the required dynamic range has to be specified accordingly. In such a perspective, even if the marine signal is drowned, and can no longer be extracted from a too high aerosol signal, the aerosol signal itself can be successfully exploited. This possibility exists if the sensor is not saturating in the presence of significant aerosol loads. The following table provides, for the main channels, the radiances that would exit an atmosphere with an aerosol optical thickness ($\tau_a$= 2, at 550 nm, in a geometry leading to the maximal signal (although outside of the sun glint zone)). In this calculation the aerosol model is of maritime type, with a relative humidity of 70%.

This maximal signal is found for a solar zenith angle of about 41° and when the viewing angle is also about 41° in the solar plane, so that the backward lobe of the aerosol phase function is directly involved in forming the (multiply scattered) exiting radiance. Note that, in such conditions, the relative contribution of the marine signal to the TOA signal is essentially zero (the ocean is not “seen” by the sensor), except for oligotrophic waters and in the blue and violet channels only (where the relative contribution does not exceed 2%, however). The following numbers are not intended to be definitive numbers, only a reasonable estimate of expected radiances in the presence of high aerosol loads.

| Channels (nm) | 410 | 443 | 560 | 710 | 750 | 865 |
|---|---|---|---|---|---|---|
| W $m^{-2}$ $sr^{-1}$ $\mu m^{-1}$ | 205 | 189 | 138 | 92 | 82 | 58 |

The above values are increased with respect to the maximum values (to be observed when the horizontal visibility is 23 km, *i.e.* in good viewing conditions), by a factor of approximately 1.4 (at 410 nm), or of 2.9 (at 865 µm); therefore the impact of implementing such a monitoring aerosol capability is more important in the NIR channels,than for the visible channels. Very likely, a bi-linear gain (such as used with SeaWiFS) or an equivalent capability will be necessary to accommodate such high radiances, without cutting down the high sensitivity required when favorable atmospheric conditions allow observation of the ocean. More recently, improved detectors, and use of multiple gains, or dual digitization, have enabled bright and dark targets to be accommodated with only a slight sacrifice of performance. This allows the sensor to be more useful for other earth science disciplines.

## 5.3 Sun glint avoidance

The illumination geometry of an Earth scene by the sun is critical for an optical remote sensor: when the sunlight reflected from the Earth's surface is too close to the main instrument axis direction, the sensor can be saturated by the received energy, so that the signal recorded becomes useless. This phenomenon, called sunglint effect, is observed primarily over water bodies, due to wave motions on the surface, which may align water facets to reflect sunlight directly toward the sensor and yield an extended sunglint pattern. The brightness of the sunglint is related to the texture of the surface, so that its changes correlate with local roughness and wave steepness, and ultimately with the local wind.

The occurrence of sunglint patterns may prevent a remote sensor from providing the complete coverage of the Earth surface required. Several solutions have been devised, to avoid or minimize the loss of data when the instrument is saturated by sunglint. Possible mechanisms for glint avoidance include tilting of the instrument away from the direct reflection of sunlight, or in general the adoption of a multi-angle viewing mode. However, because of the need to modify the sensor set-up, such mechanisms may render a certain data loss unavoidable (*e.g.*, when switching tilt direction during the equator crossings). Other dynamical avoidance mechanisms call for the use of particular scanning (*e.g.*, conical) techniques or spinning of the sensor/satellite system. Alternatively, a proper choice of orbital parameters can minimize glint recurrence and ensure coverage of contaminated areas within a reasonable time (*e.g.*, a few days). Finally, the availability of a constellation of sensors can also provide glint-free scenes, when at least two instruments can look simultaneously at the same target from different angles.

# 6. Other operational aspects

## 6.1 Ground resolution, temporal resolution, coverage

The extent of an area that can be detected by a given sensor is prescribed by its instantaneous field of view (IFOV), whereas both the spatial and temporal coverage are controlled by the orbit characteristics of the satellite, as well as the scanning capability of the sensor. In other words, the satellite and sensor properties in terms of ground resolution and temporal coverage have to be designed at an early stage of the mission configuration after agreement on the mission objectives.

Past, present and expected "low-medium resolution" ocean-colour sensors on polar-orbiting platforms have ground resolution at nadir ranging from *c.a.* 250 m to 7 km, and global coverage from 1 to 3 days (see Table 3), except for CZCS which was limited to two hours of operation each day, and MOS, not systematically operated. The absence of an on-board recording system reduces the coverage of MOS to available receiving stations. Note that the characteristics of each sensor have been selected for the monitoring of a large range of surface water phenomena, and applications in different fields, from global climate modeling to small-scale operational management in the coastal areas.

Therefore, any "standardization" or recommendation that would ensure continuity of the spatial and temporal sampling characteristics for future satellite-based ocean-colour sensors may require a trade-off between different levels of application and the technical achievement on board the satellite. As an example, global coverage at a ground resolution of 300 m is technically too demanding (high number of receiving stations or excessive storage units on board the satellite), whereas 7 km pixel resolution (*e.g.*, POLDER) may not be suitable for coastal applications.

As a compromise, recommendations for future ocean-colour sensors may be as follows:

- On-board storage of 4 km ground resolution data at global scale;

**Table 3. Spatial and temporal coverage of various ocean-colour sensors.**

| Sensor | Ground resolution (at nadir) | Recurrent period of satellite | Coverage |
|---|---|---|---|
| CZCS | 825 m | 6 days | No global coverage |
| MOS | 520 m | 24 days | No global coverage |
| OCTS | 700 m | 41 days | 3 days global coverage |
| SeaWiFS | 1.13 km | 16 days | 2 days global coverage |
| POLDER | 6 x 7 km | 41 days | 1 day quasi-global coverage |
| MODIS | 1.0 km | 16 days | 1-2 days global coverage |
| MERIS | 1.2 km / 300 m | 35 days | 3 days global coverage |
| GLI | 1.0 km / 250 m | 4 days | 3 days global coverage |

- Direct downlink of higher resolution data (1 km) on specific request for regional studies;
- Global daily coverage would be justified for coastal studies and for a sufficient representation of the cloud-covered areas;
- Even though the present experience, and the plans for immediate future, are confined to the use of polar orbiting ocean-colour sensors, there are strong arguments for a deployment of similar sensors from geostationary positions, or from low-inclination orbiting platforms, able to provide a higher frequency monitoring together with a better coverage of tropical zones (see below).

## 6.2 Data distribution, accessibility

Data acquisition and archiving are best accomplished by dedicated, specialized facilities, usually operated (either directly or under contract) by Space Agencies. As this has been the trend for quite some time, a certain degree of standardization, extended to end-users interested in having direct data acquisition capabilities, has already been achieved in this field.

In general, though, users are anticipating long-term continuity of data as inputs to scientific and (quasi) operational applications. There is a need for operational systems that provide data of proven quality and accessibility for a number of years. The experience acquired in this field has shown that the vast quantities of data generated by remote sensors, and the scientific complexities inherent in data processing (in particular for optical data) to derive environmental parameters, represent the most serious obstacles to their use. Managing and exploiting the information potential of integrated, remotely-sensed data requires that substantial efforts be made in the generation of value-added information products, and in their analysis, using specific scientific tools.

The development of specific (quasi) real time data product lines, and of corresponding historical time series – as well as dedicated algorithms and models – in support of marine environmental research and applications, are seen as pre-requisites to ensure data accessibility. Contemporary data, generated by new sensors, should be screened, selected, assembled, and banked as quality-controlled sets of derived parameters, at processing levels to be defined. The same tools developed for ingesting new data, as they become available, should be used to update the time series of historical data (possibly coupled to suitable auxiliary data, *e.g.*, atmospheric and meteo-climatic parameters), to enhance the statistical significance of the series or to open new information lines. These activities should also be accompanied by the collection and/or development of data management, processing and analysis tools, to be made available together with the data sets themselves. This is to ensure that algorithms and models (*e.g.*, site or time specific) are always available for the exploitation of the banked data.

Suitable data access and distribution means, based on electronic publishing techniques, should also be identified and implemented. Formats (for data archiving, retrieval and distribution) represent a critical issue that should be clarified by the competent organizations (*e.g.*, the Committee on Earth Observation Satellites, CEOS, *ad hoc* working group). In general, it is envisioned that such implementations should comply with the guidelines identified and/or established by current research efforts in this field (*e.g.*, the Center for Earth Observation, CEO, program at the Joint Research Center, Ispra, Italy).

## 6.3 Sensors in Geostationary Position

Ocean-colour sensors on sun-synchronous, polar orbiting satellites are capable of supplying water-leaving radiances with high spectral and spatial resolution and a revisit period of approximately two to three days. This relatively low frequency coverage, further reduced in the presence of clouds, is inadequate to study oceanic processes that occur at shorter time scales. Ocean-colour observations from geostationary platforms could be used to study processes that require several ocean-colour observations during a single day. From a geostationary position, it can be envisaged that the sensor is aimed at a restricted zone for a specific monitoring at high spatial resolution, or as well, has an all-embracing view of the planet; this second option is more adapted for a global monitoring along the line of the present document.

Geostationary satellites provide high frequency observations of the environment over large geographic regions (high latitude zones excluded) and permit the resolution of dynamic processes with time scales of hours to days. The "fixed view" of these platforms offers additional capabilities, such as providing a consistent viewing geometry to any given earth location, monitoring features that can only be detected by instruments capable of "staring", and increasing daily image coverage by compositing cloud-free areas of individual images collected during the same day. Furthermore, augmenting the continuous ocean-colour observations of geostationary platforms with the high spectral and spatial resolution data from polar orbiters will allow the investigation of oceanic processes not possible with either platform separately. Unfortunately, no current geostationary platform possesses the ability to measure ocean colour, nor is it presently considered to be a requirement by government Agencies.

The current Geostationary Operational Environmental Satellite (GOES) system, operated by the National Oceanic and Atmospheric Administration (NOAA), provides half-hourly observations of Earth-emitted and reflected radiation. Each GOES comprises two instruments: an Imager and Sounder. Together, these sensors acquire high-resolution visible and infrared data, as well as temperature and moisture profiles of the atmosphere, from which atmospheric temperature, winds, moisture, and cloud cover data can be derived. Addition of an ocean-colour capability to GOES has been discussed in the past, but with little progress. We are broaching this issue again, proposing that ocean-colour capability be added as a requirement for the next generation of geostationary platforms, GOES N-R. The European meteorological satellite (EUMETSAT) program consists of a series of geostationary spacecraft (Meteosat) continuously operating since 1977. These sensors provide images (2500 lines of 5000 pixels) in three spectral bands (thermal infrared, water vapor channel, and "VIS"); the latter channel, centered on 0.7 μm, extends from 0.3 up to 1 μm. India has also been operating a series of geostationary satellites (Insat series): the data are not, at present, available to the international community.

Adding ocean-colour bands to such instruments is technically feasible. For instance, the GOES Advanced Imager Study Review (Silver Springs, MD on August 28, 1997), in which the results of a conceptual design study of the advanced Imager based on present NOAA requirements were presented, indicated that the sensor had been under utilized. Under its current configuration, the sensor could easily incorporate a limited number of ocean-colour bands. This sentiment was echoed later in the review when it was suggested that ocean colour be added to the baseline requirements of the sensor. In addition to its technical feasibility, including ocean colour as a requirement on GOES, or Meteosat, must be justified programmatically.

There are numerous scientific reasons to promote geostationary ocean-colour observations. It must be kept in mind, however, that maintaining a rather demanding noise-equivalent radiance from a geostationary orbit results in a considerable increase in pixel size, to the extent that (for a given detector technology) the instantaneous field of view cannot be reduced considerably. Therefore the achievable geometric resolution limits the nature and spatial scale of investigation and monitoring to be envisaged, whereas the possibility of frequent acquisitions provides unquestionable advantages. In this context, such sensors in geostationary positions can be complementary of, but in no way substitute for, sensors in sun-synchronous orbits. These data will aid in addressing the following topics:

- Detecting, monitoring, and predicting noxious or toxic algal blooms of notable extension;
- Initializing and validating coastal circulation models, at mesoscale;
- Assessing the geological and biological response to storm and other short-term events (dust or smoke plumes, for instance);
- Monitoring biotic and abiotic material in transient surface features, such as extended river plumes and tidal fronts;
- Tracking hazardous materials, such as oil spills (narrow instantaneous field of view required).

Several NOAA Line Offices and agencies have stated an interest or requirement for geostationary ocean colour. The US Navy, for instance, wishes to obtain ocean-colour imagery at two-hour intervals. The Tropical Prediction Center of the National Hurricane Center may be interested in using these data to improve estimates of hurricane intensification and predict landfall. Similar interests were expressed by scientists in other countries.

If ocean colour monitoring from geostationary positions becomes a requirement, various studies will be needed to weigh tradeoffs and arrive at an acceptable design. Several potential designs exist. For instance, measurements could be made with the main GOES imager with the addition of two or three bands, or with separate focal planes, but sharing the scan mirror and telescope. Alternatively, a separate sensor could be constructed. The former appears to be the most cost-effective approach. Minimal specifications of spectral band placement, width, and signal-to-noise-ratio necessary to perform ocean-colour observations for GOES would also have to be ascertained. Calibration and radiometric stability control are also other issues to be addressed.

Geostationary ocean colour will not be available for at least another decade. NOAA or Eumetsat require approximately 10 years, from design to launch, to complete a geostationary platform. Little or no chance exists of adding ocean-colour bands on GOES-P, which is planned for launch in 2007 (launch readiness: 2006). Time is available, however, to justify and incorporate an ocean-colour requirement on the next GOES platform, Q, which is planned for launch in 2010 (launch readiness: 2008).

In summary, ocean-colour observations from a geostationary platform would complement concurrent observations from polar orbiters and permit the investigation of dynamic oceanic processes, not presently possible. Adding an ocean-colour capability on the next generation of GOES platforms appears to be scientifically tenable and technically feasible (in the authors' opinion). Inclusion of this capability as a requirement and its financial support, however, await approvals by NOAA and other involved management agencies.

## 6.4 Other Orbital Options

Other orbital options exist that can improve frequency of temporal coverage. The Taiwanese ROCSAT, for example, will be placed in a low-inclination orbit much like that of the Space Shuttle. The result is higher temporal coverage in the tropics, where coverage with sun-synchronous polar orbits is worst. This is potentially valuable, for many of the same reasons given to support geostationary observations; in particular, the coverage avoids bias because of diurnal cloud formation and sun glint in tropical regions. The disadvantage of course, shared to a lesser degree by the geostationary approach, is lack of coverage in the productive high latitude regions.

A third approach to achieving higher temporal coverage, but which preserves the high latitude view, is placement of a constellation of polar-orbiting ocean-colour sensors, offset in their respective orbital planes. A constellation of, say, eight SeaWiFS-class sensors in sun-synchronous orbits, but with differing equator-crossing times, would dramatically improve the global spatial and temporal coverage, assuming that the intercalibration issues could be adequately addressed. The approach towards low-cost, minimal sensors taken in this document would reduce the costs associated with multiple builds of identical sensors, improve the full global ocean coverage in both space and time, and provide a viable alternative to an array of geostationary observing platforms. International coordination is highly desirable in view of optimizing the capabilities of any multisensor assemblage.

# Conclusions

1. It is assumed that global and permanent monitoring of ocean colour will be considered as necessary in the near future, similar to meteorological and other oceanographic monitoring requirements. Such an operational ocean-colour program must be based on a minimum number of dedicated sensors for a complete and repetitive coverage. These sensors must be as simple and cheap as possible, albeit fulfilling the scientific requirements that allow the most important properties to be retrieved accurately, according to the present state-of-art. The minimum set of properties, important for biogeochemistry (carbon cycle), for dynamics of the upper oceanic layer, and for earth radiative budget (aerosols), are algal biomass distribution and evolution, sediment distribution and transport, and aerosol optical thickness and nature (above the oceans).

2. A constellation of sensors would be an adequate solution, operated from geostationary positions (four to five) to ensure a complete longitudinal coverage at high temporal frequency, and simultaneously from sun-synchronous polar orbits, with symmetrical modes (ascending and descending) to ensure a complete (low frequency) coverage within two to three days. Other configurations, including low latitude orbiting sensors and appropriate phasing of polar orbiting sensors could also be envisaged.

3. A certain commonality, in terms of spectral channels, already exists between the present and near-future instruments (*cf.* Fig 1); it is rather well represented by the SeaWiFS instrument (which was actually a low-cost sensor). Therefore the effort required to converge toward an identical (and minimal) set of channels does not seem excessive, and a consensus could be within reach, including an agreement about bandwidth.

4. Restricting the aim of such a mission to the monitoring of a pigment index in Case 1 waters (about 97% of the whole ocean), to sediment detection in coastal environments, and assessment of aerosols, leads to the adoption of a minimal set of five channels (the combination C2 on page 16), of which two are devoted to the atmospheric correction and aerosol monitoring (channels 744-757 and 855-890 nm), and three to determination of oceanic variables (channels 438-448, 485-495 and 550-565 nm). The detection of two or three independent variables requires, in principle, at least five channels in the visible part of the spectrum (plus two or three in the near infrared for the atmospheric correction); the corresponding algorithms for the retrieval of these three optically active substances are not yet consolidated. Therefore a less ambitious goal, albeit more realistic in the present state of knowledge, and sufficient for most of the applications listed above, leads to a minimal set of five to six channels (combination C2, as mentioned above, or better, C3, which includes an additional channel at 407-417 nm).

5. Even if simplified with respect to the number of channels, these sensors cannot be simplified in terms of several sensitive points and crucial capabilities such as:

- the radiometric accuracy, implying high signal-to-noise ratios (low noise equivalent radiances in all channels, including those in the near infra-red);

- the capability of controlling the radiometric stability (in-flight calibration involving the whole optical arrangement, and inter-calibration between sensors);
- an adequate dynamic range, able to accommodate the low oceanic signals in the case of clear atmosphere, and those, about twice higher, to be observed in the presence of relatively high aerosol loading.

6. With such an observational system, based on similar, possibly identical, instruments, it is conceivable that a common set of basic algorithms could be adopted, as well as a standardization of the deliverable products. The data exchange and management, the merging of the end products, and the distribution would be highly facilitated. Before such an operational system were decided upon, a convergence of the characteristics of the near-future sensors could be sought, as well as, if still possible, a coordination in terms of orbit phasing of these sensors, for optimized use.

**APPENDIX 1. Channel positions of various ocean-colour sensors, 1978-2000**

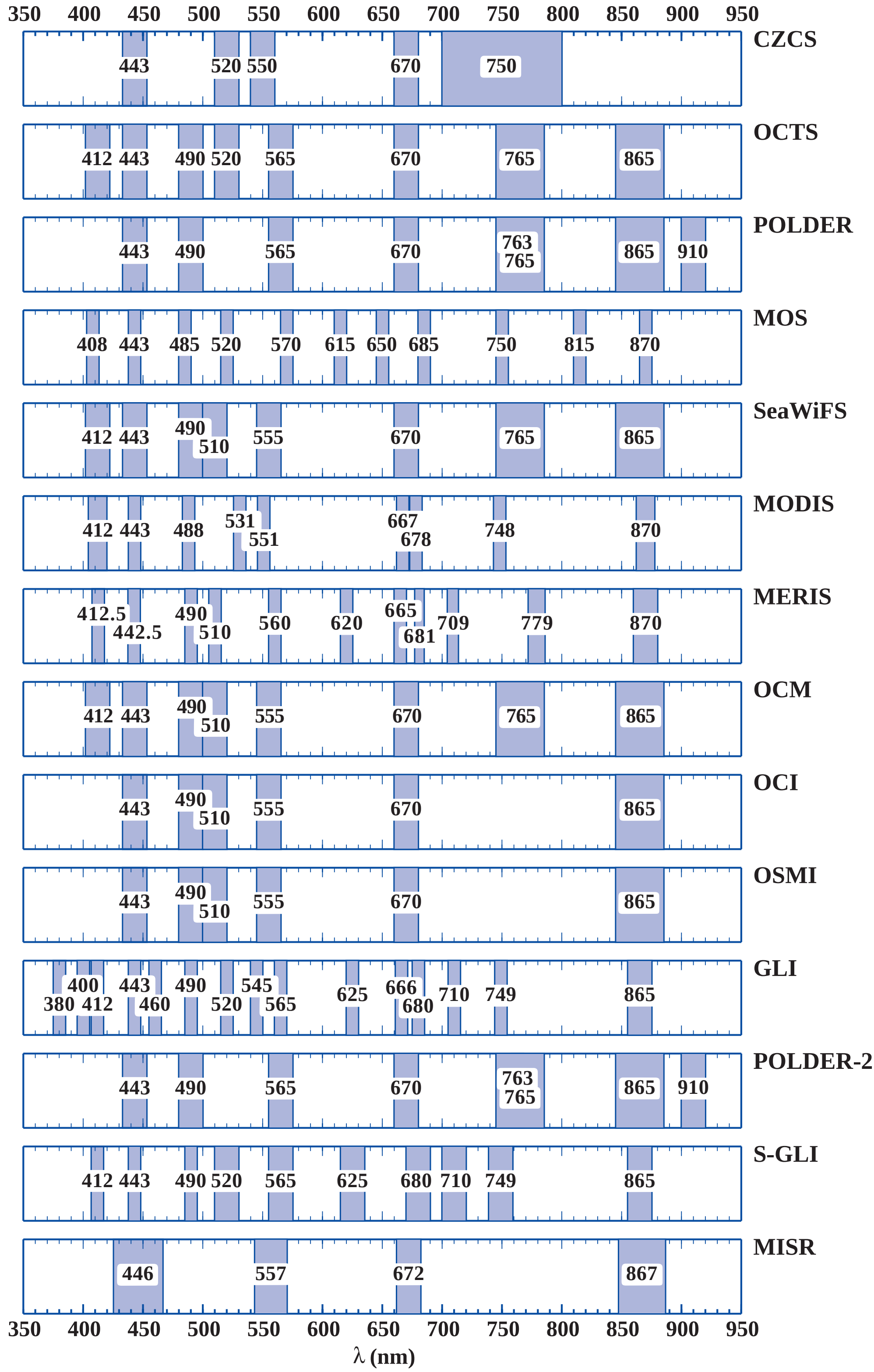

## APPENDIX II. Detailed information about the radiometric characteristics of various ocean- color sensors.

### a) CZCS

| Channel | Wavelength | Band Width | Scene Radiance | SNR : PFT | NEΔL: PFT |
|---|---|---|---|---|---|
| | nm | nm | $W\ m^{-2}\ sr^{-1}\mu m^{-1}$ | | $W\ m^{-2}\ sr^{-1}\ \mu m^{-1}$ |
| 1 | 443 | 20 | 54.2 | 260 | 0.2085 |
| 2 | 520 | 20 | 45 | 260 | 0.1731 |
| 3 | 550 | 20 | 38.6 | 233 | 0.1657 |
| 4 | 670 | 20 | 13.4 | 143 | 0.0937 |
| 5 | 750 | 100 | 10.8 | 267 | 0.0404 |
| | | | | NEΔT: PFT | |
| | μm | μm | K | K | |
| 6 | 11.5 | 2 | 270 | 0.25 | |

where SNR: PFT: Signal to Noise Ratio: Proto Flight Test

NEΔL: PFT: Noise Equivalent Radiance = Scene Radiance/SNR

Ref: Development of the Coastal Zone Colour Scanner for NIMBUS-7 , Volume 2 - Test and Performance Data. NASA Final Report F78-11, Rev. A, May 1979

**b) OCTS**

| Channel | Wavelength | Band Width | High | Low | SNR: SPC High | Low | SNR:PFT High | Low | NEΔL:PFT High |
|---|---|---|---|---|---|---|---|---|---|
| | nm | nm | W m$^{-2}$ sr$^{-1}$ μm$^{-1}$ | W m$^{-2}$ sr$^{-1}$ μm$^{-1}$ | | | | | |
| 1 | 412 | 20 | 145 | 10 | 450 | 30 | 779 | 32 | 0.1861 |
| 2 | 443 | 20 | 150 | 8 | 500 | 25 | 1373 | 41 | 0.1092 |
| 3 | 490 | 20 | 130 | 11 | 500 | 40 | 1453 | 120 | 0.0895 |
| 4 | 520 | 20 | 120 | 12 | 500 | 50 | 994 | 136 | 0.1207 |
| 5 | 565 | 20 | 90 | 8 | 500 | 40 | 988 | 126 | 0.0911 |
| 6 | 670 | 20 | 60 | 3 | 500 | 25 | 1603 | 54 | 0.0374 |
| 7 | 765 | 40 | 40 | 2 | 500 | 25 | 706 | 61 | 0.0567 |
| 8 | 865 | 40 | 20 | 2 | 450 | 45 | 637 | 70 | 0.0314 |
| | | | TST | TLW | NEΔL:SPC TST | NEΔT:PFT TLW | TST | TLW | |
| | μm | μm | K | K | K | K | K | K | |
| 9 | 3.715 | 0.33 | 300 | 250 | 0.15 | 1.4 | 0.13 | 1.34 | |
| 10 | 8.525 | 0.55 | 300 | 200 | 0.15 | 1.2 | 0.07 | 0.44 | |
| 11 | 10.85 | 1.1 | 300 | 180 | 0.15 | 1.1 | 0.09 | 0.63 | |
| 12 | 12.05 | 1.3 | 300 | 180 | 0.2 | 1.1 | 0.16 | 1.07 | |

where High: high level, Low: low level, SNR: SPC: Signal to Noise Ratio: Specification, SNR: PFT: Signal to Noise Ratio: Proto Flight Test

TST: Standard input Temperature, TLW: Low level input Temperature, NEΔL: PFT: Noise equivalent radiance = Radiance/SNR (High),

Ref: OCTS Cal/Val Document Ver. 1, NASDA/EORC May 1995

### c) POLDER

| Channel | Wavelength | Band Width | Polarization | Reflectance range High | Reflectance range Low |
|---|---|---|---|---|---|
| | nm | nm | | | |
| 1 | 443 | 20 | no | — | 0.05-0.22 |
| 2 | 443 | 20 | yes (3 angles/channels) | 0.05-1.1 | — |
| 3 | 490 | 20 | no | — | 0.034-0.17 |
| 4 | 565 | 20 | no | — | 0.019-0.11 |
| 5 | 670 | 20 | yes (3 angles/channels) | 0.1-1.1 | 0.013-0.25 |
| 6 | 763 | 10 | no | 0.07-1.1 | 0.008-0.25 |
| 7 | 765 | 40 | no | 0.07-1.1 | 0.008-0.25 |
| 8 | 865 | 40 | yes (3 angles/channels) | 0.07-1.1 | 0.008-0.25 |
| 9 | 910 | 20 | no | 0.1-1.1 | 0.007-0.25 |

Ref : ADEOS Reference Handbook (NASDA)

### c) POLDER (continued)

| Channel | Wavelength | | NE∆R Reflectance level High Dynamic Mode | | | | | NE∆R Reflectance level Low Dynamic Mode | | | | |
|---|---|---|---|---|---|---|---|---|---|---|---|---|
| | nm | Reflectance level R | 0.05 | 0.10 | 0.20 | 0.50 | 1.00 | 0.01 | 0.02 | 0.05 | 0.10 | 0.20 |
| 1 | 443 | 443NP | 0.19 | 0.25 | 0.36 | Sat. | Sat. | NA | NA | 0.19 | 0.25 | 0.36 |
| 2 | 443 | 443P | 0.44 | 0.53 | 0.68 | 1.00 | 1.38 | NA | NA | 0.44 | 0.53 | 0.68 |
| 3 | 490 | 490NP | 0.15 | 0.20 | 0.27 | Sat. | Sat. | NA | NA | 0.15 | 0.20 | 0.27 |
| 4 | 565 | 565NP | 0.10 | 0.14 | Sat. | Sat. | Sat. | NA | 0.07 | 0.10 | 0.14 | Sat. |
| 5 | 670 | 670P | 0.42 | 0.51 | 0.66 | 0.97 | 1.30 | NA | 0.11 | 0.15 | 0.20 | 0.29 |
| 6 | 763 | 763NP | 0.57 | 0.67 | 0.84 | 1.20 | 1.60 | 0.13 | 0.15 | 0.20 | 0.26 | 0.35 |
| 7 | 765 | 765NP | 0.42 | 0.51 | 0.66 | 0.97 | 1.30 | 0.09 | 0.11 | 0.16 | 0.21 | 0.29 |
| 8 | 865 | 865P | 0.42 | 0.51 | 0.66 | 0.97 | 1.30 | 0.09 | 0.11 | 0.16 | 0.21 | 0.29 |
| 9 | 910 | 910NP | 0.52 | 0.53 | 0.55 | 0.61 | 0.69 | 0.14 | 0.16 | 0.21 | 0.28 | 0.38 |

NP : Non Polarized measurement  Sat. : Saturation  P : Polarized measurement  NA : Not applicable

NE∆R: Noise Equivalent Reflectance (PFT) (x $10^3$)

### d) SeaWiFS

| Channel | Wavelength | Band Width | MAX | STR | SNR: SPC | SNR: PFT | NEΔL:PFT |
|---|---|---|---|---|---|---|---|
| | nm | nm | $W\ m^{-2}\ sr^{-1}\mu m^{-1}$ | $W\ m^{-2}\ sr^{-1}\mu m^{-1}$ | | | |
| 1 | 412 | 20 | 136.3 | 91 | 499 | 990 | 0.0919 |
| 2 | 443 | 20 | 132.5 | 84.1 | 674 | 1091 | 0.0771 |
| 3 | 490 | 20 | 105 | 65.6 | 667 | 1170 | 0.0561 |
| 4 | 510 | 20 | 90.8 | 56.4 | 640 | 1152 | 0.0490 |
| 5 | 555 | 20 | 74.4 | 45.7 | 596 | 1069 | 0.0428 |
| 6 | 670 | 20 | 42 | 24.6 | 442 | 781 | 0.0315 |
| 7 | 765 | 40 | 30 | 16.1 | 455 | 859 | 0.0187 |
| 8 | 865 | 40 | 21.3 | 10.9 | 467 | 726 | 0.0150 |

where
- MAX: Saturation Radiance
- STR: Standard Radiance
- SNR:SPC: Signal to Noise Ratio: Specification
- SNR: PFT: Signal to Noise Ratio: Proto Flight Test
- NEΔL: PFT: Noise Equivalent Radiance = STR/SRN:PFT

Ref: Barnes, R.A., Barnes, W.L., Easias, W.E., and McClain, C.R.: Prelaunch Acceptance Report for the SeaWiFS Radiometer, NASA, December 1996. SeaWiFS Technical Report Series Volume 22.

**e) MODIS**

| Channel | Wavelength | Band Width | Spectral Radiance | SNR: SPC* | NEΔL | Primary Use |
|---|---|---|---|---|---|---|
| | nm | nm | W $m^{-2}$ $sr^{-1}$ $\mu m^{-1}$ | | W $m^{-2}$ $sr^{-1}$ $\mu m^{-1}$ | |
| 1 | 645 | 50 | 21.8 | 128 | 0.1703(250 m) | Land/Cloud |
| 2 | 858.5 | 35 | 24.7 | 201 | 0.1229(250 m) | Boundaries |
| 3 | 469 | 20 | 35.3 | 243 | 0.1453(500 m) | Land/Cloud Properties |
| 4 | 555 | 20 | 29 | 228 | 0.1272(500 m) | |
| 5 | 1240 | 20 | 5.4 | 74 | 0.0730(500 m) | |
| 6 | 1640 | 24 | 7.3 | 275 | 0.0265(500 m) | |
| 7 | 2130 | 50 | 1 | 110 | 0.0091(500 m) | |
| 8 | 412.5 | 15 | 44.9 | 933 | 0.0484 | Ocean colour/Phytoplankton/ |
| 9 | 443 | 10 | 41.9 | 1325 | 0.0317 | Biogeochemistry |
| 10 | 488 | 10 | 32.1 | 1308 | 0.0247 | |
| 11 | 531 | 10 | 27.9 | 1385 | 0.0183 | |
| 12 | 551 | 10 | 21 | 1114 | 0.0189 | |
| 13 | 667 | 10 | 9.5 | 1163 | 0.0082 | |
| 14 | 678 | 10 | 8.7 | 1265 | 0.0069 | |
| 15 | 748 | 10 | 10.2 | 1077 | 0.0095 | |
| 16 | 869.5 | 15 | 6.2 | 1000 | 0.0062 | |
| 17 | 915 | 30 | 10 | 167 | 0.0599 | Atmospheric Water Vapor |
| 18 | 936 | 10 | 3.6 | 57 | 0.0632 | |
| 19 | 940 | 50 | 15 | 250 | 0.0600 | |

* (Except for channels 8-16, for which SNR - PFT values are provided.)

**e) MODIS (continued)**

| Channel | Wavelength | Band Width | Spectral Radiance | NE∆T | SNR | Primary Use |
|---|---|---|---|---|---|---|
| | nm | nm | W $m^{-2}sr^{-1}\mu m^{-1}$ | K | | |
| 20 | 3.75 | 0.18 | 0.45 | 0.05 | | Surface/Cloud Temperature |
| 21 | 3.959 | 0.6 | 2.38 | 2 | | |
| 22 | 3.959 | 0.6 | 0.67 | 0.07 | | |
| 23 | 4.05 | 0.06 | 0.79 | 0.07 | | |
| 24 | 4.465 | 0.065 | 0.17 | 0.25 | | Atmospheric temperature |
| 25 | 4.515 | 0.067 | 0.59 | 0.25 | | |
| 26 | 1.375 | 0.03 | 6 | — | 150 | Cirrus Cloud/Water Vapor |
| 27 | 6.715 | 0.36 | 1.16 | 0.25 | | |
| 28 | 7.325 | 0.3 | 2.18 | 0.25 | | |
| 29 | 8.55 | 0.3 | 9.58 | 0.05 | | |
| 30 | 9.73 | 0.3 | 3.69 | 0.25 | | Ozone |
| 31 | 11.03 | 0.5 | 9.55 | 0.05 | | Surface/ Cloud Temperature |
| 32 | 12.02 | 0.5 | 8.94 | 0.05 | | |
| 33 | 13.335 | 0.3 | 4.52 | 0.25 | | Cloud top altitudes/ Atmospheric profiles |
| 34 | 13.635 | 0.3 | 3.76 | 0.25 | | |
| 35 | 13.935 | 0.3 | 3.11 | 0.25 | | |
| 36 | 14.235 | 0.3 | 2.08 | 0.35 | | |

Ref : Barnes *et al.* (1998); Esaias *et al.* (1998)

**f) MERIS**

| Channel | Wavelength | Band Width | *LST | SNR: PFT | NEΔL |
|---|---|---|---|---|---|
| | nm | nm | $W\ m^{-2}\ sr^{-1}\ \mu m^{-1}$ | | |
| 1 | 412.5 | 10 | 47.9 | 1871 | 0.0256 |
| 2 | 442.5 | 10 | 41.9 | 1650 | 0.0254 |
| 3 | 490 | 10 | 31.2 | 1418 | 0.0220 |
| 4 | 510 | 10 | 23.7 | 1222 | 0.0194 |
| 5 | 560 | 10 | 18.5 | 1156 | 0.0160 |
| 6 | 620 | 10 | 12.0 | 863 | 0.0139 |
| 7 | 665 | 10 | 9.2 | 708 | 0.0130 |
| 8 | 681.25 | 7.5 | 8.3 | 589 | 0.0141 |
| 9 | 709 | 9 | 6.9 | 631 | 0.0111 |
| 10 | 753.75 | 7.5 | | | |
| 11 | 760 | 2.5 | | | |
| 12 | 779 | 14 | 4.9 | 628 | 0.0078 |
| 13 | 870 | 20 | 3.2 | 457 | 0.0070 |
| 14 | 890 | 10 | | | |
| 15 | 900 | 10 | | | |

* Typical L values (sun zenith angle 60°, visibility 23 km, aerosol of the maritime type, ozone 350 DU, water vapor 2 g cm-2; the sub-satellite point is at 58.6°N, the day number is 80, the pixel is at the center of the field of view, and the chlorophyll concentration is 0.3 mg m-3). The NEΔL are for the reduced spatial resolution mode (1.2 km x 1.2 km)

Channels 10 and 11 - $O_2$ bands; Channels 14 and 15 - $H_2O$, Vegetation

## g) GLI

| Channel | Wavelength | Band Width | LST | LMX Ocean | LMX Land/Atmosphere | SNR: SPC | SNR:EM | NE$\Delta$L:EM |
|---|---|---|---|---|---|---|---|---|
| | nm | nm | W $m^{-2}sr^{-1}\mu m^{-1}$ | W $m^{-2}sr^{-1}\mu m^{-1}$ | W $m^{-2}sr^{-1}\mu m^{-1}$ | | | |
| 1 | 380 | 10 | 59 | — | 365 | 600 | 779 | 0.0757 |
| 2 | 400 | 10 | 70 | 139 | — | 800 | 1373 | 0.0510 |
| 3 | 412 | 10 | 65 | 130 | — | 800 | 1453 | 0.0447 |
| 4 | 443 | 10 | 54 | 109 | 560 | 800 | 994 | 0.0543 |
| 5 | 460 | 10 | 54 | 108 | 624 | 800 | 988 | 0.0547 |
| 6 | 490 | 10 | 43 | 86 | — | 800 | 1603 | 0.0268 |
| 7 | 520 | 10 | 31 | 64 | 539 | 600 | 706 | 0.0439 |
| 8 | 545 | 10 | 28 | 56 | 549 | 600 | 637 | 0.0440 |
| 9 | 565 | 10 | 23 | 47 | — | 800 | 1262 | 0.0182 |
| 10 | 625 | 10 | 17 | 33 | — | 800 | 996 | 0.0171 |
| 11 | 666 | 10 | 13 | 26 | — | 800 | 863 | 0.0151 |
| 12 | 680 | 10 | 12 | 24 | — | 800 | 853 | 0.0141 |
| 13 | 678 | 10 | 12 | — | 438 | 200 | 260 | 0.0462 |
| 14 | 710 | 10 | 10 | 18 | — | 700 | 826 | 0.0121 |
| 15 | 710 | 10 | 10 | — | 311 | 250 | 300 | 0.0333 |
| 16 | 749 | 10 | 7 | 14 | — | 550 | 684 | 0.0102 |
| 17 | 763 | 8 | 6 | — | 350 | 130 | 164 | 0.0366 |
| 18 | 865 | 20 | 5 | 9 | — | 450 | 739 | 0.0068 |
| 19 | 865 | 10 | 5 | — | 304 | 130 | 151 | 0.0331 |
| 20 | 460 | 70 | 36 | — | 624 | 200 | 284 | 0.1268 |
| 21 | 545 | 50 | 25 | — | 549 | 150 | 221 | 0.1131 |
| 22 | 660 | 60 | 14 | — | 150 | 100 | 202 | 0.0693 |
| 23 | 825 | 110 | 21 | — | 257 | 140 | 334 | 0.0629 |
| 24 | 1050 | 20 | 8 | — | 203 | 300 | 359 | 0.0223 |
| 25 | 1135 | 70 | 8 | — | 200 | 350 | 366 | 0.0219 |
| 26 | 1240 | 20 | 5.4 | — | 138 | 70 | 355 | 0.0152 |
| 27 | 1380 | 40 | 1.5 | — | 94 | 120 | 149 | 0.0101 |
| 28 | 1640 | 200 | 5 | — | 69 | 109 | 268 | 0.0187 |
| 29 | 2210 | 220 | 1.3 | — | 30 | 105 | 129 | 0.0101 |

**g) GLI (continued)**

| Channel | Wavelength | Band Width | TST | TLW | NEΔT:SPC TST | TLW | NEΔT:EM TST | TLW |
|---|---|---|---|---|---|---|---|---|
| | μm | μm | K | K | K | K | K | K |
| 30 | 3.715 | 0.33 | 300 | 250 | 0.15 | 1.8 | 0.15 | 1.4100 |
| 31 | 6.7 | 0.5 | 300 | 200 | 0.1 | 1.5 | 0.07 | 1.1500 |
| 32 | 7.3 | 0.5 | 300 | 200 | 0.1 | 1 | 0.07 | 0.8500 |
| 33 | 7.5 | 0.5 | 300 | 200 | 0.1 | 1 | 0.07 | 0.7600 |
| 34 | 8.6 | 0.5 | 300 | 180 | 0.1 | 0.5 | 0.03 | 0.4900 |
| 35 | 10.8 | 1 | 300 | 180 | 0.1 | 0.5 | 0.06 | 0.4300 |
| 36 | 12 | 1 | 300 | 180 | 0.1 | 0.5 | 0.09 | 0.4800 |

where LST: Standard Input Radiance

LMX: Maximum Radiance

SNR: SPC: Signal to Noise Ratio : Specification

SNR: EM: Signal to Noise Ratio : Engineering Model Test

TST: Standard Input Temperature

TLW: Low Level Input Temperature

NEΔL: PFT: Noise equivalent radiance = LST/SNR

Ref:ADEOS-II/GLI CDR document (in Japanese) Fujitsu Lim. January, 1997

### h) S-GLI

| Channel | Wavelength | Band Width | LST | LMX | SNR: SPC | NEΔL:SPC | |
|---|---|---|---|---|---|---|---|
| | nm | nm | W m$^{-2}$sr$^{-1}$µm$^{-1}$ | W m$^{-2}$sr$^{-1}$µm$^{-1}$ | | | |
| **Ocean Colour Imager (OCI)** | | | | | | | |
| 1 | 412 | 10 | 65 | 130 | 800 | 0.0813 | |
| 2 | 443 | 10 | 54 | 109 | 800 | 0.0675 | |
| 3 | 490 | 10 | 43 | 86 | 800 | 0.0538 | |
| 4 | 520 | 20 | 31 | 64 | 600 | 0.0517 | |
| 5 | 565 | 20 | 23 | 47 | 800 | 0.0288 | |
| 6 | 625 | 20 | 17 | 33 | 800 | 0.0213 | |
| 7 | 680 | 20 | 12 | 24 | 1000 | 0.0120 | |
| 8 | 710 | 20 | 7 | 14 | 1000 | 0.0070 | |
| 9 | 749 | 20 | 7 | 14 | 800 | 0.0088 | |
| 10 | 865 | 20 | 5 | 9 | 800 | 0.0063 | |
| **Atmospheric and Land Imager (ALI)** | | | | | | | |
| 1 | 380 | 10 | 60 | 400 | 500 | 0.1200 | |
| 2 | 400 | 10 | 60 | 400 | 500 | 0.1200 | |
| 3 | 443 | 10 | 50 | 600 | 800 | 0.0625 | |
| 4 | 460 | 10 | 50 | 650 | 800 | 0.0625 | |
| 5 | 545 | 20 | 30 | 550 | 600 | 0.0500 | |
| 6 | 678 | 20 | 23 | 450 | 400 | 0.0575 | |
| 7 | 710 | 20 | 20 | 350 | 400 | 0.0500 | |
| 8 | 763 | 8 | 6 | 350 | 400 | 0.0150 | |
| 9 | 865 | 20 | 5 | 304 | 400 | 0.0125 | |
| 10 | 460 | 50 | 40 | 624 | 400 | 0.1000 | (250 m) |
| 11 | 545 | 50 | 25 | 549 | 400 | 0.0625 | (250 m) |
| 12 | 678 | 50 | 15 | 250 | 400 | 0.0375 | (250 m) |
| 13 | 865 | 50 | 20 | 257 | 400 | 0.0500 | (250 m) |
| 14 | 940 | 20 | 10 | 200 | 400 | 0.0250 | (250 m) |
| 15 | 1050 | 20 | 8 | 203 | 400 | 0.0200 | (250 m) |

**h) S-GLI (continued)**

| Channel | Wavelength | Band Width | LST | LMX | SNR: SPC | NEΔL:SPC | |
|---|---|---|---|---|---|---|---|
| | μm | μm | | | | | |
| **Infrared Imager (IRI)** | | | | | | | |
| 1 | 1.24 | 0.02 | 5 | 138 | 400 | 0.0125 | |
| 2 | 1.38 | 0.04 | 1.5 | 94 | 400 | 0.0038 | |
| 3 | 1.64 | 0.2 | 5 | 69 | 400 | 0.0125 | (250 m) |
| 4 | 2.21 | 0.1 | 1.3 | 30 | 400 | 0.0033 | (250 m) |
| | | | | | **NEΔT:SPC** | | |
| | **μm** | **μm** | **TST** | **TLW** | **TST** | **TLW** | **TMX** |
| 1 | 3.7 | 0.3 | 300 | 250 | 0.1 | 0.5 | 340 |
| 2 | 6.7 | 0.5 | 300 | 200 | 0.1 | 0.5 | 340 |
| 3 | 7.3 | 0.5 | 300 | 200 | 0.1 | 0.5 | 340 |
| 4 | 7.4 | 0.5 | 300 | 200 | 0.1 | 0.5 | 340 |
| 5 | 8.6 | 0.5 | 300 | 180 | 0.1 | 0.5 | 340 |
| 6 | 10.8 | 0.7 | 300 | 180 | 0.1 | 0.5 | 340 |
| 7 | 12 | 0.7 | 300 | 180 | 0.1 | 0.5 | 340 |

where LST: Standard Input Radiance

LMX: Maximum Radiance

SNR: SPC: Signal to Noise Ratio : Specification

TST: Standard Input Temperature

TLW: Low Level Input Temperature

NEΔL: PFT: Noise Equivalent Radiance = LST/SNR

Ref: T. Nakajima (Private communication)

## References

Åas, E. 1987. Two-stream irradiance model for deep waters. *Appl. Optics,* **26:** 2095-2101.

Ackelson, S. G., Balch, W. M. and Holligan, P. M. 1994. Response of water-leaving radiance to particulate calcite and chlorophyll-*a* concentrations: A model for Gulf of Maine coccolithophore blooms. *J. Geophys. Res.,* **99:** 7483-7499.

Babin, M., Morel, A. and Gentili, B. 1996. Remote sensing of sea surface sun-induced chlorophyll fluorescence: consequences of natural variations in the optical characteristics of phytoplankton and the quantum yield of chlorophyll-*a* fluorescence. *Int. J. Remote Sensing,* **17:** 2417-2448.

Balch, W. M., Kilpatrick, K. A., Holligan, P. M. and Trees, C. 1996. The 1991 coccolithophore bloom in the central north Atlantic. I: Optical properties and factors affecting their distribution *Limnol. Oceanogr.,* **41:** 1669-1683.

Barnes, W. L., Pagano, T. S. and Salomonson, V. V. 1998. Prelaunch characteristics of the Moderate Resolution Imaging Spectroradiometer (MODIS) on EOS-AMI. IEEE *Trans. Geosci. Remote Sensing.* 36: 1088-1100

Bidigare, R. R., Morrow, J. H. and Kiefer, D. A. 1989. Derivative analysis of spectral absorption by photosynthetic pigments in the western *Sargasso Sea. J. Mar. Res.,* **47:** 323-341.

Bricaud, A. and Morel, A. 1987. Atmospheric corrections and interpretation of marine radiances in CZCS imagery: use of a reflectance model. *Oceanol. Acta, Symposium Proceedings:* 33-50.

Bricaud, A. and Stramski, D. 1990. Spectral absorption coefficients of living phytoplankton and nonalgal biogenous matter: A comparison between the Peru upwelling area and the Sargasso Sea. *Limnol. Oceanogr.,* **35:** 562-583.

Bricaud, A., Babin, M., Morel, A. and Claustre, H. 1995. Variability in the chlorophyll-specific absorption coefficients of natural phytoplankton: Analysis and parameterization. *J. Geophys. Res.,* **100:** 13,321-13,332.

Brown, C. and Yoder, J. A. 1994. Coccolithophorid blooms in the global ocean. *J. Geophys. Res.,* **99:** 7467-7482.

Chisholm, S. W., Olson, R. J., Zettler, E. R., Goericke, R., Waterbury, J. B. and Welschmeyer, W. A. 1988. A novel free-living prochlorophyte abundant in the oceanic euphotic zone. *Nature,* **334:** 340-343.

Cleveland, J. S. 1995. Regional models for phytoplankton absorption as a function of chlorophyll-*a* concentration. *J. Geophys. Res.,* **100:** 13,333-13,344.

Dowell, M. and Hoepffner, N. 1997. Reflectance modeling in case II waters: contamination of the elastic signal by CDOM fluorescence. *Proc. International Workshop on MOS-IRS and Ocean Colour* (Berlin, 28-30 April 1997).

Esaias, W. E., Abbott, M. R., Barton, I., Brown, O. B., Campbell, J. W., Carder, K. L., Clark, D. K., Evans, R. L., Hodge, F. E., Gordon, H. R., Balch, W. P., Letelier, R., Minnet, P. J. 1998. An Overview of MODIS capabilities for Ocean Science observations. *IEEE Trans. Geosci. Remote Sensing.* 36: 1250-1265

Fischer, J. 1985. On the information content of multispectral radiance measurements over an ocean. *Int. J. Remote Sensing,* **6:** 773-786.

Fischer, J., Doerffer, R. and Grassl, H. 1986. Factor analysis of multispectral radiances over 0coastal and open ocean water based on radiative transfer calculations. *Appl. Optics,* **25:** 448-456

Frouin, R., Schwindling, M. and Deschamps, P-Y. 1996. Spectral reflectance of sea foam in the visible and near infrared: In situ measurements and remote sensing implications and aerosols. *J. Geophys. Res.*, **101:** 14,361-14,371.

Garver, S. A., Siegel, D. A. and Mitchell B.G. 1994. Variability in near-surface particulate absorption spectra: What can a satellite ocean colour imager see? *Limnol. Oceanogr.*, **39:** 1349-1367.

Gege, P. 1997. Characterization of the phytoplankton in Lake Constance for classification by remote sensing. *Arch. Hydrobiol.* In press.

Gordon, H. R. 1979. Diffuse reflectance of the ocean: the theory of its augmentation via chlorophyll-*a* fluorescence at 685 nm. *Appl. Optics,* **18:** 1161-1166

Gordon, H. R., Brown, O. B. and Jacobs, M. M. 1975. Computed relationships between the inherent and apparent optical properties of a flat, homogeneous ocean. *Appl. Optics,* **14:** 417-427.

Gordon, H. R., Brown, O. B., Evans, R. H., Brown, J. W., Smith, R. C., Baker, K. S. and Clarke, D. K. 1988. A semianalytic radiance model of ocean colour. *J. Geophys. Res.*, **93:** 10,909-10,924.

Gordon, H. R., 1997. Atmospheric correction of ocean colour imagery in the Earth Observing System era. *J. Geophys. Res.*, **102:** 17,081-17,106.

Gower, J. F. R. and Borstad, G. 1981. Use of *in vivo* fluorescence line at 685 nm for remote sensing surveys of surface chlorophyll-*a*. In: *Oceanography from Space*, J. F. R. Gower edit., New York Plenum Press, pp. 329-338.

Haltrin, V. I., Kattawar, G. W. and Weidemann, A. D. 1997. Modeling of elastic and inelastic scattering effects in ocean optics. In: *Ocean Optics XIII. Proc. SPIE,* **2963:** 597-602.

Hawes, S. K., Carder, K. L. and Harvey, G. R. 1992. Quantum fluorescence efficiencies of fulvic and humic acids: effect on ocean colour and fluorometric detection. In: *Ocean Optics XI, Proc. SPIE,* **1750:** 212-223.

Hoepffner, N. and Sathyendranath, S. 1991. Effect of pigment composition on absorption properties of phytoplankton. *Mar. Ecol. Prog. Ser.*, **73:** 11-23.

Hoepffner, N. and Sathyendranath, S. 1992. Bio-optical characteristics of coastal waters: Absorption spectra of phytoplankton and pigment distribution in the western North Atlantic. *Limnol. Oceanogr.*, **37:** 1660-1679.

Hoepffner, N. and Sathyendranath, S. 1993. Determination of the major groups of phytoplankton pigments from the absorption spectra of total particulate matter. *J. Geophys. Res.*, **98:** 22,789-22,803.

Kirk, J. T. O. 1981. Monte Carlo study of the nature of the underwater light field in, and the relationships between optical properties of, turbid yellow waters. *Aust. J. Freshwater Res.*, **32:** 517-532.

Letelier, R.M. and Abbott, M.R. 1996. An analysis of chlorophyll fluorescence algorithms for the Moderate Resolution Imaging Spectrometer (MODIS). *Rem. Sens. Environ.*, **58:** 215-223.

Lee, Z., Carder, K. L., Hawes, S. K., Steward, R. G., Peacock, T. G. and Davis, C. O. 1994. Model for the interpretation of hyperspectral remote-sensing reflectance. *Appl. Opt.*, **33:** 5721-5732.

Mitchell, B. G. and Kiefer, D. A. 1988. Variability in pigment specific particulate fluorescence and absorption spectra in the north-eastern Pacific Ocean. *Deep-Sea Res., (Part A)*, **35:** 665-689.

Morel, A. and Prieur, L. 1977. Analysis of variations in ocean colour. *Limnol. Oceanogr.*, **22:** 709-722.

Morel, A. and Bricaud, A., 1981. Theoretical results concerning light absorption in a discrete medium, and application to specific absorption of phytoplankton. *Deep-Sea Res., (Part A),* **28:** 1375-1393.

Morel, A. 1988. Optical modeling of upper ocean in relation to its biogenous matter content (Case 1 waters). *J. Geophys. Res.,* **93:** 10,749-10,768.

Morel, A., Ahn, Y-H., Partensky, F., Vaulot, D. and Claustre H. 1993. *Prochlorococcus and Synechococcus:* A comparative study of their optical properties in relation to their size and pigmentation. *J. Mar. Res.,* **51:** 617-649.

Morel, A. 1997. Consequences of a Synechococcus bloom upon the optical properties of oceanic (Case 1) waters. *Limnol. Oceanogr.,* **42:** In Press.

Mueller , J. L. and Austin, R. W., 1995. Ocean Optics protocols for SeaWiFS validation. Revision 1. *NASA Tech. Memo.,* **Vol. 25:** 66pp.

Neville, R. A. and Gower, J. F. R. 1977. Passive remote sensing of phytoplankton via chlorophyll-*a* fluorescence. *J. Geophys. Res.,* **82:** 3487-3493.

Roesler, C. S., Perry, M. J. and Carder K. L. 1989. Modeling in situ phytoplankton absorption from total absorption spectra in productive inland marine waters. *Limnol. Oceanogr.,* **34:** 1510-1523.

Rothman, L. S., Gamache, R. R., Goldman, A., Brown, L. R., Toth, R. A., Pickett, H. M., Poynter, R. L., Flaud, J.-M., Camy-Peyret, C., Barbe, A., Husson, N., Rinsland, C. P. and Smith, A. H. 1987. The HITRAN database: 1986 edition. *Appl. Optics,* **26:** 4058-4097.

Rothman, L. S., Gamache, R. R., Tipping, R. H., Rinsland, C. P. and Smith, M. A. 1992. The HITRAN molecular database: Editions of 1991 and 1992. *J. Quant. Spectrosc. Radiat. Transfer,* **48:** 469-507.

Sathyendranath, S., Prieur, L. and Morel, A. 1989. A three-component model of ocean colour and its application to remote sensing of phytoplankton pigments in coastal waters. *Int. J. Remote Sensing,* **10:** 1373-1394.

Sathyendranath, S. Hoge, F. E., Platt, T. and Swift, R. N. 1994. Detection of phytoplankton pigments from ocean colour: improved algorithms. *Appl. Optics,* **33:** 1081-1089.

Sathyendranath, S. and Platt, T. 1997. Analytic model of ocean colour. *Appl. Optics,* **36:** 2620-2629.

Sosik H. M., Chisholm, S. W. and Olson R. J. 1989. Chlorophyll fluorescence from single cells: Interpretation of flow cytometric signals. *Limnol. Oceanogr.,* **34:** 1749-1761.

Stavn, R. H. 1990. Raman scattering effects at the shorter wavelengths in clear ocean waters. In: *Ocean Optics X. Proc. SPIE,* **1302:** 94-100.

Stavn, R. H. 1992. External factors and water Raman scattering in clear ocean waters: skylight, solar angle, and the air/water interface. In: *Ocean Optics XI. Proc. SPIE,* **1750:** 138-148.

Subramaniam, A. and Carpenter, E. J. 1994. An empirically derived protocol for the detection of blooms of the marine cyanobacterium *Trichodesmium* using CZCS imagery. *Int. J. Remote Sensing,* **15:** 1559-1569.

Sugihara S., Kishino, M. and Okami, N. 1984. Contribution of Raman scattering to upward irradiance in the sea. *J. Oceanogr. Soc. Japan,* **40:** 397-403.

Viollier, M. and Sturm, B. 1984. CZCS data analysis in turbid coastal water, *J. Geophys. Res.,* **89:** 4977-4985.

Yentsch, C. S. and Phinney, D. A. 1985. Spectral fluorescence: an ataxonomic tool for studying the structure of phytoplankton populations. *J. Plankt. Res.*, **7:** 617-632.

Wernand, M. R., Schimwell, S. J. and de Munk, J. C. 1997. A simple method of full spectrum reconstruction by a five-band approach for ocean colour applications. *Int. J. Remote Sensing* 18: 1977-1986.

## List of Acronyms and Abbreviations

| | |
|---|---|
| ALI | Atmospheric and Land Imager |
| CEO | Center for Earth Observation |
| CEOS | Committee on Earth Observation Satellites |
| CNES | Centre National d'Etudes Spatiales |
| CZCS | Coastal Zone Colour Scanner |
| DLR | German Aerospace Center |
| EM | Engineering Model Test |
| EOS | Earth Observing System |
| ESA | European Space Agency |
| EUMESTAD | European Meteorological Satellite |
| FWHM | Full Width at Half Maximum |
| GLI | Global Imager |
| GLOBEC | Global Ocean Ecosystems Dynamics |
| GOES | Geostationary Operational Environmental Satellite |
| HITRAN | High-resolution Transmission Molecular Absorption Database |
| IFOV | Instantaneous Field of View |
| IGBP | International Geosphere-Biosphere Programme |
| IOCCG | International Ocean Colour Coordinating Group |
| IRI | Infrared Imager |
| IRS | Indian Remote-Sensing Satellite |
| ISRO | Indian Space Research Organization |
| JGOFS | Joint Global Ocean Flux Study |
| KARI | Korean Aerospace Research Institute |
| LMX | Maximum Radiance |
| LST | Standard Input Radiance |
| LOICZ | Land-Ocean Interactions in the Coastal Zone |
| $(L_w)_N$ | Normalized Water-leaving Radiance |
| MERIS | Medium Resolution Imaging Spectrometer |
| MISR | Multi-angle Imaging SpectroRadiometer |
| MODIS | Moderate Resolution Imaging Spectroradiometer |
| MOS | Modular Optoelectric Scanner |
| NASA | National Aeronautics and Space Administration |
| NASDA | National Space Development Agency of Japan |
| $NE\Delta L$ | Noise Equivalent Radiance |
| $NE\Delta R$ | Noise Equivalent Reflectance |
| $NE\Delta T$ | Noise Equivalent Temperature |
| NIR | Near Infrared part of the Spectrum |
| NOAA | National Oceanic and Atmospheric Administration |

| | |
|---|---|
| OCI | Ocean Colour Imager |
| OCM | Ocean Colour Monitor |
| OCTS | Ocean Colour and Temperature Scanner |
| OSC | Orbital Sciences Corporation |
| OSMI | Ocean Scanning Multispectral Imager |
| PFT | Proto Flight Test |
| POLDER | Polarization and Directionality of the Earth's Reflectances |
| R | Reflectances |
| SeaWiFS | Sea-viewing Wide Field-of-view Sensor |
| SNR | Signal to Noise Ratio |
| SPC | Specification |
| STR | Standard Radiance |
| TLW | Low Level Input Temperature |
| TOA | Top of the Atmosphere |
| TST | Standard Input Temperature |
| UV | Ultra Violet |